Title

High-throughput single telomere analysis using DNA microarray and fluorescent in situ hybridization.

Journal

Nucleic Acids Research, 52(19)

Authors

Zheng, Yun-Ling
Wu, Xingjia
Williams, Madeline
et al.

Publication Date

2024-10-28

DOI

10.1093/nar/gkae812

Peer reviewed

Nucleic Acids Research, 2024, **52**, e96
https://doi.org/10.1093/nar/gkae812
Advance access publication date: 18 September 2024
Methods

High-throughput single telomere analysis using DNA microarray and fluorescent in situ hybridization

Yun-Ling Zheng [1,*], Xingjia Wu [1], Madeline Williams [1], Simon Verhulst [2], Jue Lin [3], Yusuke Takahashi [4], Jian-Xing Ma [4] and Ying Wang [5]

[1]Cancer Prevention and Control Program, Department of Oncology, Georgetown University Medical Center, Georgetown University, Washington, DC 20057, USA
[2]Groningen Institute for Evolutionary Life Sciences, University of Groningen, Groningen, The Netherlands
[3]Department of Biochemistry and Biophysics, University of California San Francisco, San Francisco, CA 94143, USA
[4]Department of Biochemistry, Wake Forest School of Medicine, NC 27157, USA
[5]TelohealthDx, LLC, Clarksburg, MD 20871, USA

*To whom correspondence should be addressed. Tel: +1 202 687 6654; Fax: +1 202 687 7505; Email: yz37@georgetown.edu

Abstract

The human telomere system is highly dynamic. Both short and long leucocyte average telomere lengths (aTL) are associated with an increased risk of cancer and early death, illustrating the complex relationship between TL and human health and the importance of assessing TL distributions with single TL analysis. A DNA microarray and telomere fluorescent *in situ* hybridization (DNA-array-FISH) approach was developed to measure the base-pair (bp) lengths of single telomeres. On average 32000 telomeres were measured per DNA sample with one microarray chip assaying 96 test DNA samples. Various telomere parameters, i.e. aTL and the frequency of short/long telomeres, were computed to delineate TL distribution. The intra-assay and inter-assay coefficient of variations of aTL ranged from 1.37% to 3.98%. The correlation coefficient (r) of aTL in repeated measurements ranged from 0.91 to 1.00, demonstrating high measurement precision. aTLs measured by DNA-array-FISH predicted aTLs measured by terminal restriction fragment (TRF) analysis with *r* ranging 0.87–0.99. A new accurate and high-throughput method has been developed to measure the bp lengths of single telomeres. The large number of single TL data provides an opportunity for an in-depth analysis of telomere dynamics and the complex relationship between telomere and age-related diseases.

Graphical abstract

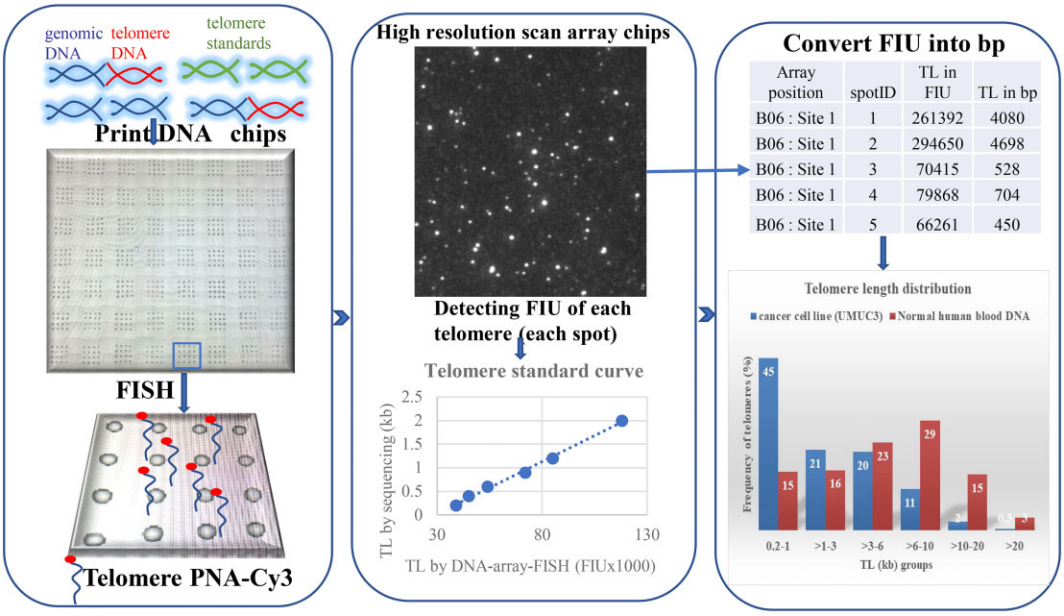

Received: April 6, 2024. **Revised:** August 30, 2024. **Editorial Decision:** September 3, 2024. **Accepted:** September 9, 2024

Introduction

The critical role of telomere length (TL) at the chromosomal ends in cell fate decisions and biological functions ranging from aging to carcinogenesis has been well established (1–6). In vertebrates, telomeres are composed of a long double-stranded array of TTAGGG repeats bound by the six-protein sheltering complex (7,8). Telomeres have an essential role in ensuring that the natural ends of chromosomes are not mistaken for sites of DNA damage. Due to the inability of the DNA replication machinery to fully replicate linear DNA (known as the end replication problem), telomeres progressively shorten with each cell division in telomerase negative cells (9–12). Critically short, or dysfunctional telomeres trigger cellular growth arrest that drive progressive atrophy and aging-associated pathologies (13,14). Deficiency in telomere function is broadly related to multiple aging-associated diseases (15–18). Short telomere length has been implicated as a risk factor in pulmonary disease (19–21), diabetes mellitus (22–24), liver cirrhosis (25,26), osteoporosis (27,28), kidney disease (29,30), Alzheimer's disease (31,32), cardiovascular disease (33,34), and cancer (35,36). Together, these diseases affect a large proportion of the U.S. adult population (18).

Results from previous studies using average TL (aTL) to test a host of hypotheses related to the biology of human aging and carcinogenesis have been inconsistent. The literature on the associations between stress (37,38), environmental exposures (39–41), disease susceptibility (34,42–45), and aTL is somewhat contradictory and the extent to which divergent findings are due to TL measurement error is unclear. TL shows considerable variability between species, individuals, tissue types and chromosome arms (46–49). By relying on aTL as the only TL characterization, these previous studies failed to consider the heterogeneity of TLs across chromosomal arms and/or among cells for a given tissue type (46–49). In fact, it is increasingly recognized that the deleterious effects of telomeres are mediated by the load of critically short telomeres (50–54) or long telomeres (55–59). For example, genetic studies in mice have shown that the shortest telomeres, rather than the aTL, are the major cause of age-related pathologies (50). The load of short TL can increase due to the gradual shortening of telomeres during normal cellular aging or as a result of catastrophic telomere loss (60–62). Therefore, determining the load of short telomeres and TL distribution is critical to further advance the understanding of the role of telomeres in aging and cancer.

Various methods have been developed for the measurement of TL using cells or genomic DNA samples and generally only provide information on aTL (53,63–66). TL can be measured by quantitative fluorescence *in situ* hybridization (Q-FISH) methods, including metaphase Q-FISH and interphase Q-FISH. Metaphase Q-FISH can detect TL from each chromosomal end (49), which requires dividing cells as well as a skilled cytogeneticist; it is very labor intensive (53,64). Flow cytometry-based FISH (Flow-FISH) can estimate the aTL of interphase nuclei of white blood cells (67). It can measure aTL of sub-types of leucocytes, but requires expensive equipment and is labor intensive. The high cost and labor-intensive nature of these methods limits their applications in large scale population studies.

Methods that have been applied to analyze purified genomic DNA samples include terminal restriction fragment (TRF) analysis (68), quantitative PCR (qPCR) (69), multiplex luminex assay (70), digital PCR (71), single-telomere length analysis (STELA) (46,72), telomere shortest length assay (TeSLA) (73), peptide nucleic acid (PNA) hybridization and analysis of single telomeres (PHAST) (74), Nano Pore (75–77) and PacBio HiFi long read sequencing (78). TRF analysis estimates the aTL from the intensity and size distribution of the 'telomeric smear' by Southern blot analysis (68). It requires a large amount of starting genomic DNA (6 μg) and is an insensitive method to detect the shortest telomeres (<3 kb). Using ligation and PCR amplification of telomeres in combination with Southern blot analysis, STELA and TeSLA can provide information about the abundance of the shortest telomeres (46,73). However, both methods are limited to amplify telomeres that are shorter than 8 kb (STELA) or 18 kb (TeSLA). Eight PCR reactions are typically set up to assay one DNA sample and the number of telomeres being amplified with 8 PCR reactions is limited to a few hundreds, limiting the precision of estimated the TL distribution. While PHAST is able to generate high-resolution TL measurements, it is labor intensive and requires specialized equipment and software that is not commercially available. Recently published single-telomere length analysis using Nano pore or PacBio HiFi long read sequencing demonstrated telomere length analysis at the nucleotide resolution (75–78). However, this method requires a large amount of starting genomic DNA (10–40 μg) and complex pre-sequencing enrichment of telomeric DNA and library preparation steps, and is labor-intensive and expensive (75–78).

The quantitative PCR (qPCR) TL measurement method is the only method that has been widely adopted in large scale epidemiological studies due to its high-throughput and low-cost nature. The qPCR method measures the ratio of telomere signal (T) to a single copy gene signal (S) and provides only T/S ratios as the relative aTL quantitation which is assay-specific, therefore cannot be compared between studies with an independent 'yardstick'. The qPCR method is not suitable for quantifying aTL for cancer cells since most cancer cells are aneuploidy that affects T/S ratios (79). There are concerns about the validity and reliability of the qPCR TL measurement method in population studies. It has been shown that qPCR is sensitive to protocol deviations, often associated with high measurement errors, and assay precision varies widely across laboratories (80–82), highlighting the need to develop a new method for accurate TL measurement for large human population studies.

We report here the development of a novel method for single telomere length analysis utilizing DNA microarray and fluorescent *in situ* hybridization (DNA-array-FISH). This new approach enables the measurement of telomere length in base pair (bp) of individual telomeres in a high-throughput manner. Notably, it can detect telomeres as short as 200 bp with a dynamic range spanning from 0.1 to 340 kb. Furthermore, each microarray chip can analyze 96 DNA samples, and multiple DNA microarray chips can be assayed in a single FISH experiment. We conducted a comparison of aTLs from 92 human blood samples using both DNA-array-FISH and TRF methods and demonstrated the high precision and accuracy of DNA-array-FISH for TL measurements.

Materials and methods

Generation of telomeric size standards

TL standards were generated through a repeated extension process as previously described (74). Briefly, a telom-

ere template of 90 bp was synthesized, with restriction enzymes KpnI and XhoI sites at the 5′ end and SalI at the 3′ end (GGTA CCTCGAGGG-(TTAGGG)$_{15}$-TCGAC) (Integrated DNA Technologies, Inc. Coralville, IW). Two additional forward (5′ -TGGTACCTCGAGGGTTAGG-3′) and reverse (5′-GTCGACCCTAACCCTAACC-3′) primers that can anneal to the telomere template at both ends were used in a PCR reaction to create a double-stranded telomere template of 100 bp. The telomere template was then ligated into a pCR4-TOPO TA vector (Life Technologies, Grand Island, NY) following the manufacturer's instructions, and verified by Sanger DNA sequencing. The telomere template insert was then released from the TA vector by XhoI and SalI digestion and cloned into the XhoI site of the pUC19 vector (New England Biolabs, Ipswich, MA). The pUC19 plasmid containing the telomeric insert was then digested with XhoI and served as a subsequent hosting vector. To prepare the telomere insert for extension, the cloned telomeric inserts in the pUC19 plasmid was released with KpnI and SalI and mixed with the hosting vector. It was then fused together using the Gibson Assembly cloning kit (New England Biolabs, Ipswich, MA) to extend the telomeric insert in the hosting vector, following the manufacturer's instructions. This process was repeated several times to obtain plasmids containing the desired sizes of telomeric inserts. For instance, a vector hosting a 100 bp telomeric sequence was fused with a 200 bp telomeric fragment to produce a plasmid clone containing a 300 bp telomeric insert. Plasmid clones containing telomeric inserts sized 200, 300, 400, 600, 900, 1200, 2000 and 2400 bp were successfully obtained. The size of the telomere inserts was confirmed by Sanger DNA sequencing and by digestion with XhoI and SalI to release the telomeric inserts, followed by gel electrophoresis.

DNA extraction and evaluation of DNA integrity

DNA samples were purified using the Puregene DNA extraction kit or QiAmp blood mini kit (Qiagen, Germantown, MD) according to the manufacturer's instructions. We utilized the same standards as required by the Southern blot-based TRF method to evaluate DNA integrity (see Figure 2 in Reference #68). DNA integrity was verified by agarose gel electrophoresis and visualized with a SYBRE green dye stain (Supplementary Figure S1). DNA samples that appeared as a single compact crown-shaped band migrating in parallel with the other samples on the gel were accepted for telomere length analysis. However, a sample that appears as a smear or has a forward shift in its crown in comparison with other samples (Supplementary Figure S1, lanes 1, 3 and 5) is degraded and unsuitable for single telomere analysis by our method because degraded DNA, i.e. degraded telomere molecules, will inflate the frequency of short telomeres and lead to inaccuracies in estimated aTL.

Digestion of genomic DNA

Prior to DNA microarray construction, genomic DNA was digested with a different combination of the restriction enzymes, either *HinfI* & *RsaI*, *HinfI* & *AluI*, *HinfI* & *MnlI* or *HphI* & *MnlI*. All the restriction enzymes were purchased from New England Biolabs, Ipswich, MA. In a 96-well plate, 9.0 μl (0.5–1.0 μg) of DNA and 1.2 μl of master mixture (1 μl of 10× NEB buffer 4 plus 2 units of each enzyme) were added to each well. The plate was sealed with a cover film and incubated at 37°C for 2 h.

DNA microarray chip construction

The principle of the DNA-array-FISH method for single telomere analysis is illustrated in Figure 1. Two μl of digested genomic DNA was transferred into a 384-well PCR plate, and then 2 μl of 2× printing buffer (6× SSC and 3.0 M of Betaine) was added to each well and mixed well by repeated pipetting. The DNA samples were printed on an aminosilane coated glass slide (SCHOTT North America Inc, Louisville, KY) using a Xact II microarray printer (LabNext, Inc. West New York, NJ) with a 300-micron pin under 50–70% humidity at room temperature. Each chip/slide hosts 112 DNA samples (7 rows × 16 columns = 112 clusters) and each DNA array cluster contains 16 spots in a 4 × 4 arrangement (Figure 1A and B). The DNA chips were kept in a clean box at room temperature for 5–7 days before telomere fluorescent *in situ* hybridization (T-FISH).

DNA immobilization and telomere fluorescent *in situ* hybridization

The DNA chips were baked at 65°C overnight, cooled down to room temperature for 20 min and exposed to UV light in a UV cross-linker at an energy setting of 400 mJ/cm^2. The DNA chips were incubated with pre-hybridization/blocking buffer (5× SSC, 0.1% SDS, 1 mg/ml BSA and 50% formamide) at 42°C for 1 h, washed in deionized water for 2 min each, repeated 5 times and then dried by centrifugation at 200 × g for 1 min. Thirty microliters of hybridization buffer (50% formamide, 10 mM Tris pH 7.5, 3% blocking reagent, 1× Denhart's solution) containing 20–30 nM of the Cy3 labeled telomere specific gamma peptide nucleic acid (PNA, Cy3-O-TTA*GGGT*TAGGG, *=miniPEG gamma) probe was added to each chip and covered under a glass cover slip (24 × 50 mm). The array chips were placed in a Hybrex hybridization chamber, denatured at 75°C for 5 min and hybridized at 30°C for 3 h in a Hybrex incubator (SciGene Inc., Sunnyvale, CA). After hybridization, the array chips were washed in 2× SSC at 45°C for 10 min and 1× SSC at 45°C for 10 min, and then dried by centrifugation at 200 × g for 1 min. The array chips were mounted in an anti-fade mounting medium (Vector Laboratories Inc., Newark, CA) and stored at 4°C in the dark.

DNA array chip scanning and image analysis

The array chips were scanned using a high-content-imaging system (ImageXpress Micro 4, Molecular Device, San Jose, CA) under a 60× oil objective with an exposure time of 400 ms. Approximately 1792 images (one image per array spot, Figure 1C) were obtained per array chip. The digitized images went through a quality control process to remove poor quality images, i.e. images that were out of focus or contained debris. Within the MetaExpress software package (Molecular Device, San Jose, CA), a journal was developed to automatically analyze the images to count the number of telomeres (fluorescent spots, Figure 1D) and measure the total fluorescent intensity of each telomere. The journal uses a custom-built telomere module with background subtraction between 300 and 600, area sum minimum of 0.4, area sum maximum of 10, and round shape factor of 0.80 to

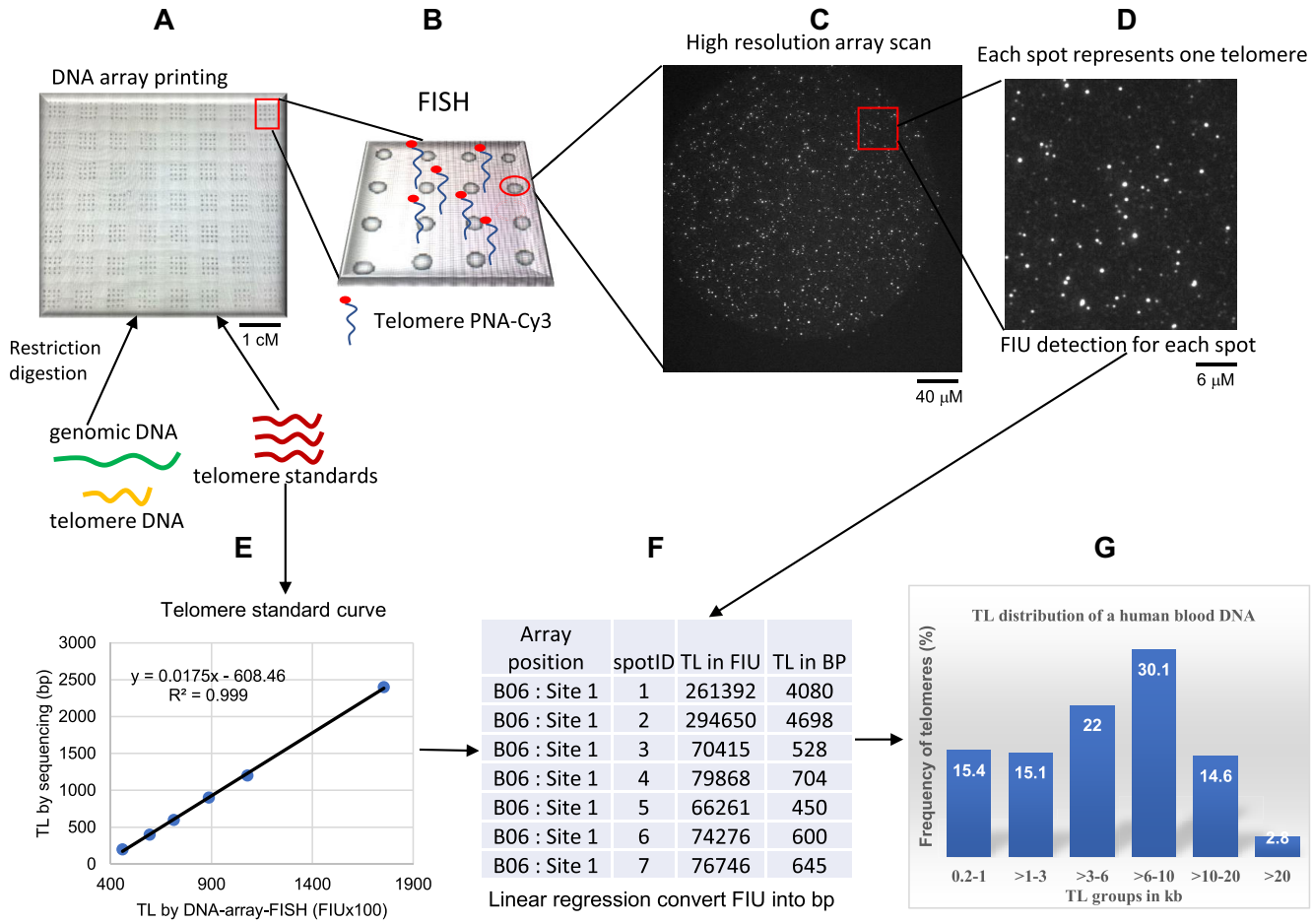

Figure 1. Schematic overview of the DNA-Array-FISH-based single telomere analysis workflow. (**A**) genomic DNA was digested with restriction enzymes and printed on amino-saline coated glass slides to make DNA microarray chips. (**B**) DNA chips were hybridized with a telomere specific PNA probe. (**C**) An array spot was scanned using a fluorescent microscopy image system under 60× oil objective. (**D**) Enlarged view of telomere signals. (**E**) A telomere standard curve. (**F**) Total fluorescent intensity of each telomere spot in the digitized images were quantified and converted into bp length using linear regression, based on the slope and intercept of the telomere standard curve. (**G**) TL distribution of a human genomic DNA.

exclude overlapping telomeres, telomere doublets, large debris, or very small background signals. The total fluorescent intensity units (FIU) of each telomere were recorded and exported into a text file. R package (version 4.1.3) was used to read and clean the data, generate a standard curve (Figure 1E) and perform telomere length conversion (from FIU to bp, Figure 1F) using linear regression models as described below.

Establish standard curve and aTL of the control DNA sample

Telomere standard curve microarray chips (SCchip) were designed and analyzed to (i) establish and optimize telomere FISH (T-FISH) condition; (ii) obtain intercept and slope values for converting FIUs into bps by linear regression and (iii) obtain aTL for the control DNA (conDNA) sample to calculate the normalization factor (N), which is used in the linear regression model to adjust for assay variations across different chips. SCchips contain cloned telomere standards sized 200, 400, 600, 900, 1200, 2000 and 2400 bp. Each SCchip contains 10 SCs and 8 replicates of a control DNA sample with known TRF-determined aTL. Length in bp of each telomere is estimated using the following linear regression model:

$$TL^{i(bp)} = [slope^{*}TL^{i(FIU)} + intercept]^{*} N,\ where N$$
$$= aTL\ of\ conDNA^{SCchip} \div aTL\ of\ conDNA^{testchip}$$

SCchips were analyzed to determine the acceptance or rejection of each tested T-FISH condition and should be examined whenever the T-FISH condition changes, such as the introduction of a new hybridization buffer or a new batch of telomere probe. The mean intercept and slope values calculated from 30 SCs (3 SCchips × 10 SC per SCchip) were used in the linear regression model for TL conversion for all test chips assayed in the same accepted T-FISH condition. The mean aTL of the control DNA from the 3 corresponding SCchips is used for calculating the N factor. Two mean SC slope and intercept values (SC0923 and SC1023, Table 1) were used to generate data for this report due to the change of telomere probe concentration. An example of a telomere SC is shown in Figure 1E and examples of images of telomere size standards are shown in Supplementary Figure S2.

Table 1. Telomere standard curve (SC) parameters and aTL of control DNA

Name of SC	Slope	Intercept	R^2	conDNA SCchip aTL[a] (bp)	conDNA TRF aTL (bp)
SC0923	0.0318	−802	0.97	7760	7611
SC1023	0.0215	−653	0.98	7671	7611

[a]aTL was estimated by telomere standard curve of the SCchip using linear regression

Quality control and quality assurance (QC/QA) consideration of TL measurement by DNA-array-FSH

Image quality

The images to be included in the analysis must be in focus and free of debris that cannot be filtered out by the telomere image analysis module.

Telomere standard curve

For any quantitative FISH-based assay, high hybridization efficiency (~100%) is required to achieve high assay precision. The SCchips containing the smallest telomeres (200 bp) are ideal for optimizing the hybridization conditions. Suboptimal hybridization conditions will lead to loss of small telomere signals and the standard curve could fail to meet the pre-set QC standards, i.e. slope <0.035 and explained variance $R^2 > 0.95$. In addition to generating intercept and slope for TL conversion, standard curves play an important role in normalizing hybridization variations between batches of chips assayed at different times. Thus, a high-quality telomere standard curve (slope < 0.0350 and $R^2 > 0.95$) is the precondition for the acceptance of a specific T-FISH condition to be applied to test chips.

Control of T-FISH hybridization variations

There are potentially three levels of assay variations: between batches of chips that were hybridized at different times, among chips within a batch, and among the cluster positions within a chip. Three QC/QA parameters were designed to minimize these variations: (i) converting TL from FIU to bp using the telomere SC slope and intercept values generated from SCchips to minimize assay variations between batches of chips assayed at different times; (ii) N factor minimizes FISH variations between chips; (iii) each DNA sample is assayed in triplicates (three chips) or quadruplicates (four chips) to reduce measurement error. If the CV of aTL among the triplicates is ≤15%, then the measurement is accepted. The average of the replicate measurements was accepted as the final TL measurement.

The sensitivity and dynamic range of DNA-array-FISH

The dynamic range of the assay is determined by the dynamic range of the digital camera used for quantitative fluorescent signal detection. When imaging bright (long telomeres) and dim (short telomeres) signals in the same acquisition, a high dynamic range is essential for maintaining linear quantitative measurements and detecting weak signals without saturating bright signals. We found that cloned telomere fragments of 0.1 kb were detectable using the ImageExpress Micro 4 high-content-imaging system under the pre-defined exposure condition. The ImageExpress Micro 4 is equipped with a 4.66-megapixel (2160 × 2160) scientific complementary metal-oxide-semiconductor (sCMOS) camera with >3 log dynamic range. It maintains linearity theoretically when capturing TL signals ranging from 0.1 to 340 kb. This dynamic range exceeds what is necessary to capture all TL signals in normal human blood cells. Our survey of 92 human blood samples revealed a mean maximal TL of 50.6 kb and that 2.9% of telomeres are longer than 20 kb (Figure 2).

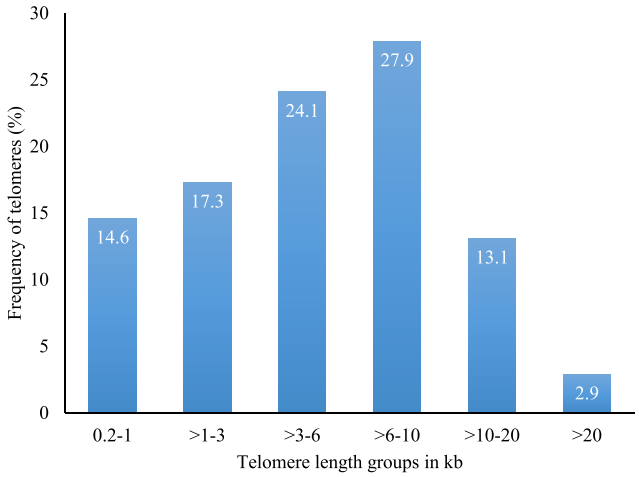

Figure 2. Average telomere length distribution of 92 human blood samples. Telomere length was measured by DNA-array-FISH with *HinfI* & *MnlI* digested DNA.

Telomere parameters generated by DNA-array-FISH

For each DNA sample, a total number of >9000 telomeres (average 32 000) were measured (samples with <9000 telomeres will be repeated). The large number of individual telomere data permits detailed examination of TL distribution. We defined seven telomere parameters that we considered useful as examples: (i) aTL, i.e. aTL^{1kb} is the average telomere length for telomeres that are longer than 1 kb (using 1 kb as cut off), or aTL^{2kb} (using 2 kb as cut off). aTL^{2kb} is used for normal human genomic DNA (blood or tissue). aTL^{1kb} is used for cancer cell lines. (ii) Frequency of telomeres in five TL groups, i.e. 1–3, >3–6, >6–10, >10–20 and >20 kb. (iii) Telomere length variation (TLV), defined as the CV of all measured telomeres that are longer than 2 kb. Other example telomere parameters include TL at percentiles of the within-sample distribution, aTL in a pre-defined percentile range etc., depending the hypotheses to be tested. Controls and telomere variables recommended for routine applications in a research setting are listed in the supplementary material (Supplementary Note 1). It's important to note that these recommendations are based on our current experiences and will be further refined by future large-scale population studies that we are actively pursuing.

Data analysis

Student *t*-test was used to compare the means of telomere parameters between repeated measurements and between different restriction digestions. Co-efficient of variation (CV) was calculated to estimate the intra- and inter-assay variation among repeated measurements. Pearson correlation (*r*)

Table 2. Effect of restriction enzyme digestion on TL measurement

	Mean (SD)	Mean (SD)	Frequency of telomeres, %, Mean (SD)				
Enzyme pair	aTL, bp	TLV, %	1–3 kb	>3–6 kb	>6–10 kb	>10–20 kb	>20 kb
HinfI & *RsaI*	7381 (975)	58.22 (3.78)	22.03 (4.22)	24.06 (4.97)	30.57 (4.17)	18.08 (4.60)	5.26 (3.04)
AluI & *HinfI*	7026 (1129)	57.29 (3.44)	21.19 (3.15)	26.50 (6.18)	31.37 (3.27)	16.48 (5.72)	4.46 (3.22)
HinfI & *MnlI*	6267 (948)	58.75 (4.21)	28.59 (3.50)	29.37 (5.24)	27.08 (2.35)	12.03 (5.17)	2.93 (2.11)
HphI & *MnlI*	6243 (995)	58.71 (3.22)	28.40 (3.96)	29.62 (5.42)	27.02 (2.79)	12.08 (5.39)	2.89 (2.24)
Pearson correlation, *r*							
HR: AH	0.88	0.87	0.68	**0.94**	0.86	0.89	0.84
HR: HpM	0.86	0.87	0.17	0.85	0.27	0.79	0.87
HR: HM	0.84	0.82	0.09	0.82	0.26	0.76	0.85
AH: HpM	**0.93**	**0.93**	0.70	**0.90**	0.57	**0.91**	**0.94**
AH: HM	**0.94**	**0.95**	0.68	**0.90**	0.55	**0.92**	**0.97**
HM: HpM	**0.97**	**0.96**	**0.97**	**0.96**	**0.97**	**0.97**	**0.97**
Paired Student *t*-test, *P*-value							
HR: AH	0.26	0.38	0.44	0.14	0.47	0.30	0.38
HR: HpM	**<0.01**	0.64	**<0.01**	**<0.01**	**<0.01**	**<0.01**	**<0.01**
HR: HM	**<0.01**	0.66	**<0.01**	**<0.01**	**<0.01**	**<0.01**	**<0.01**
AH: HpM	**0.02**	0.15	**<0.01**	0.07	**<0.01**	**0.01**	0.06
AH: HM	**0.02**	0.20	**<0.01**	0.10	**<0.01**	**0.01**	0.07
HM: HpM	0.93	0.97	0.87	0.88	0.93	0.98	0.95

DNA samples stored at -80°C freezer for 12 years were used ($N = 24$).
AH = *AluI* & *HinfI*, HM = *HinfI* & *MnlI*, HpM = *HphI* & *MnlI*, HR = *HinfI* & *RsaI*.
Bolded correlation coefficients are ≥0.90 and *p*-values are statistically significant.

was used to estimate the reproducibility of repeated measurements or between TRF and DNA-array-FISH measurements. Intraclass correlation co-efficient (ICC) estimates were calculated using the R-package rptR (83). ICC estimates vary between 0 and 1, with 0 indicating no correlation (zero precision) and 1 indicating a perfect correlation (maximum precision) between different measurements. Linear regression was used to estimate the rate of TL change by age. All reported *P*-values are two sided. The statistical analysis was carried out using R packages (version 4.1.3) (84).

Results

Effect of restriction enzyme digestion on TL measurement

Restriction enzyme digestion was carried out prior to DNA microarray chip construction. This step improves the uniformness of DNA distribution within array spots, reduces the thickness of the DNA layer on the glass surface and largely eliminates overlapping telomeres/telomere aggregates. Five frequent cutters of restriction enzymes, including *AluI, Hinf I, HpHI, MnlI* and *RsaI*, were evaluated. Previous studies have demonstrated that the combination of *HinfI* & *RsaI* or *HpHI* & *MnlI* achieved good digestion of human genomic DNA with peak bands <800 bp on a gel (68). These two pairs of enzyme mixtures are frequently used in TRF-based telomere length measurements.

We evaluated the restriction enzyme digestion using a set of 25 DNA samples that were extracted using the FlexiGene DNA kit and have been stored at −80°C for 12 years. Four enzyme pairs (*HinfI* & *RsaI, AluI* & *HinfI, HinfI* & *MnlI* or *HphI* & *MnlI*) were evaluated. One DNA sample failed digestion by all four enzyme pairs. Table 2 presents pair-wise comparisons for all four enzyme pairs. Notably, identical results were generated between enzyme pairs *HinfI* & *MnlI* and *HphI* & *MnlI* for all seven telomere parameters evaluated (Table 2 and Figure 3), indicating that these two enzyme pairs are interchangeable for the assay. The high correlations of telomere parameters (*r* ranges 0.96–0.97) between these two enzyme-pairs suggest very high within-chip measurement precision of this method. Enzyme pairs *HinfI* & *RsaI* and *AluI* & *HinfI* showed similar results except that the aTL of *HinfI* & *RsaI* digested DNA is about 350 bp longer than aTL of *AluI* &*HinfI* digested DNA ($P = 0.26$, Table 2). There are no significant differences in mean TLV among four pairs of restriction enzymes. However, significant differences were observed in aTL, frequency of telomeres in each of the five TL groups, i.e. 1–3, >3–6, >6–10, >10–20 and >20 kb, between *HinfI* & *RsaI* and *HinfI* & *MnlI* or *HphI* & *MnlI* digested DNA (Table 2). Overall aTL of *HinfI* & *RsaI* digested DNA is 1.1 kb longer than aTL of *HinfI* & *MnlI* or *HphI* & *MnlI* digested DNA. Comparing *AluI* & *HinfI* and *HinfI* & *MnlI* or *HphI* & *MnlI* digested DNA showed a similar pattern of significant differences (Table 2). Regardless of which enzyme pairs were used to digest the DNA, aTL and TLV are highly correlated between the 4 enzyme pairs tested (*r* ranges 0.84–0.97, Table 2), while variable correlations were observed for the frequency of telomeres of the five TL groups (r ranges from 0.09 to 0.97, Table 2).

The precision of DNA-array-FISH for TL measurement

Impact of array cluster position and restriction enzyme digestion on TL measurement precision

To evaluate the effect of array cluster positions on the measurement precision, one DNA sample was digested with an enzyme pair and printed on three whole chips. This experiment was repeated for four enzyme pairs (*HinfI* & *RsaI, AluI* & *HinfI, HinfI* & *MnlI* or *HphI* & *MnlI*). The mean aTL is 8196, 7659, 6793 and 7009 bp for *HinfI* & *RsaI, AluI* & *HinfI, HinfI* & *MnlI* or *HphI* & *MnlI* digested DNA, respectively (Table 3). The overall measurement variation (CV) of aTL is 5.66%, 3.21%, 3.98% and 2.60% for *HinfI* & *RsaI, AluI* & *HinfI, HinfI* & *MnlI* or *HphI* & *MnlI* digested DNA, respectively (Table 3). There are no significant differences in measurement variations when comparing the clus-

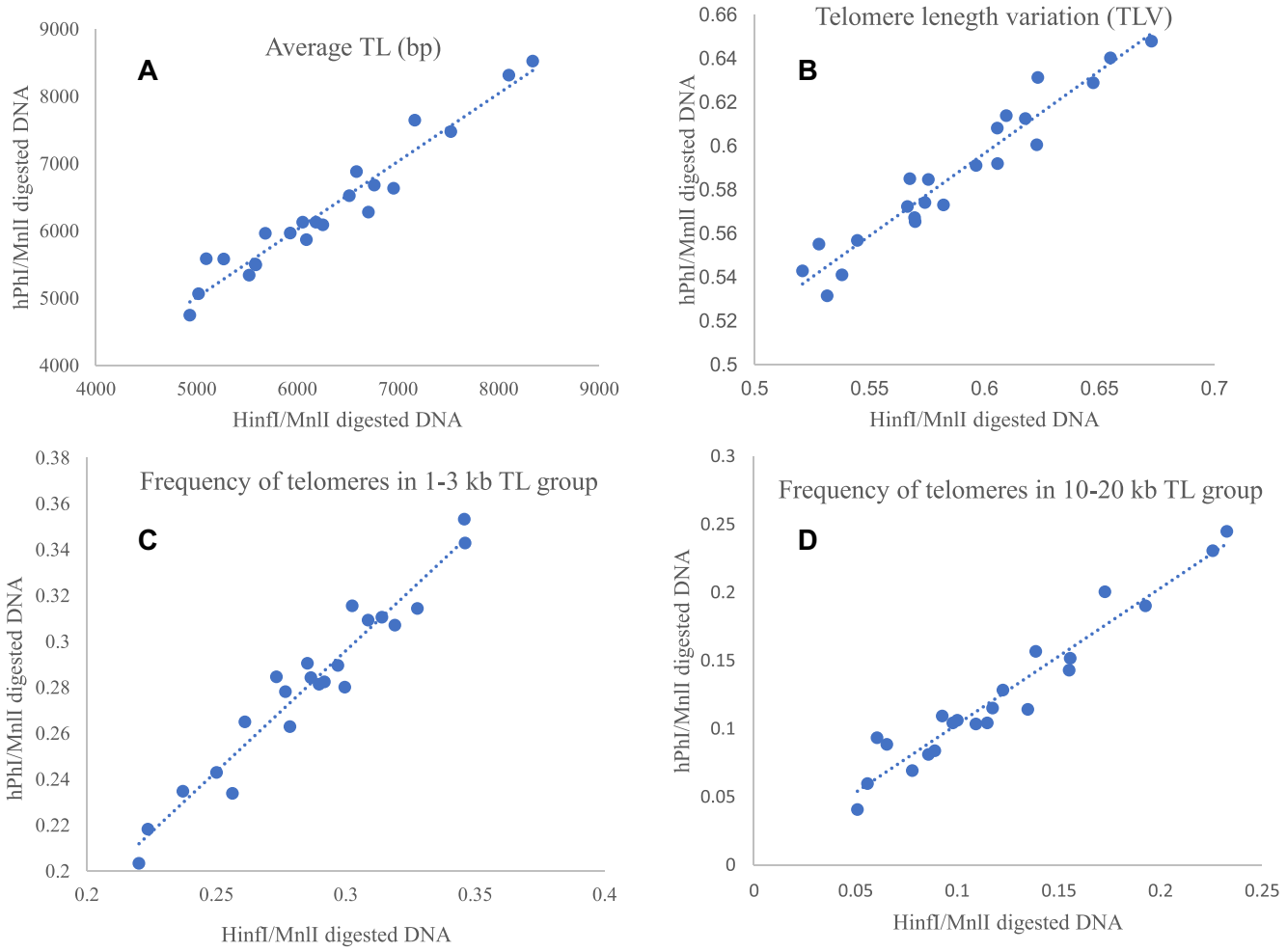

Figure 3. Correlation of telomere parameters between *HinfI* & *MnlI* and *hPhI* & *MnlI* digested DNA of human blood samples ($N = 24$). (**A**) aTL in bp, $r = 0.97$; (**B**) telomere length variation (CV), $r = 0.96$; (**C**) telomere frequencies in 1–3 kb TL group, $r = 0.97$; (**D**) telomere frequencies in 10–20 kb TL group, $r = 0.97$.

ters located at the edge, including A1–A16, G1–G16, B1–F1 and B16–F16, with inner clusters (clusters located at least one cluster away from the edges). The overall CV of TLV is 2.82%, 2.47%, 1.39% and 1.50% for *HinfI* & *RsaI*, *AluI* & *HinfI*, *HinfI* & *MnlI* or *HphI* & *MnlI* digested DNA, respectively (Table 3). There are no significant differences in TLV measurement variation when comparing the edge clusters with inner clusters. We observed higher measurement variations (CV > 10%) for the frequency of telomeres in two TL groups (1–3 and >20 kb, Table 3). Overall measurement variation for the frequency of telomeres varies greatly, with CV across a chip ranging 6.42–28.03%, 4.77–15.62%, 1.38–21.93% and 3.78–13.39% for *HinfI* & *RsaI*, *AluI* & *HinfI*, *HinfI* & *MnlI* or *HphI* & *MnlI* digested DNA, respectively (Table 3). There were no noticeable differences and trends in measurement variations of telomere frequency when comparing the edge clusters to the inner clusters. Our data indicate that *HinfI* & *RsaI* digestion is associated with longer aTL and higher measurement variation (CV = 5.66%) compared with the other three enzyme pairs (CV < 4%). The performance of *HinfI* & *MnlI* and *HphI* & *MnlI* are identical, but *HinfI* is a lower cost enzyme than *HphI*, thus *HinfI* & *MnlI* is the preferred enzyme choice for the DNA-array-FISH assay.

To evaluate inter-assay variation, three DNA samples with relatively short, medium and long TL were assayed repeatedly at different time points (at least one month apart), using *HinfI* & *MnlI* digestion. The inter-assay CV of aTL ranged between 1.37% - 3.41% and the inter-assay CV of TLVs ranged between 6.91% AND 9.24% (Table 4). The inter-assay variations for the frequency of telomeres in all TL groups were somewhat smaller than the intra-assay variations, with CV ranging between 2.42% AND 14.19% (Table 4). These data confirmed the high precision of DNA-array-FISH for the measurement of aTL in DNA samples extracted from human blood.

Reproducibility of DNA-array-FISH for TL measurement

To examine the reproducibility of the DNA-array-FISH method, we analyzed a bladder cancer cell line (UMUC3) with overexpression of the TERC gene (85) twice at different times. TL of UMUC3^{TERC} increases during *in vitro* culturing. The cells were harvested at seven passages (p0–p6) after the infection of a lentiviral construct that overexpresses TERC. DNA was extracted using the Puregene genomic DNA kit and digested with *HinfI* & *MnlI* restriction enzymes. The mean aTL of seven passages (p0 – p6) is 6179 bp and 6177 bp for assay 1 and assay 2, respectively ($P = 0.99$,

Table 3. Impact of restriction enzyme digestion and cluster position on TL measurement of one human genomic DNA

		HinfI & *RsaI*						
		Telomere parameters		Frequency of telomeres, %				
		aTL (bp)	TLV, %	1–3 kb	>3–6 kb	>6–10 kb	>10–20 kb	>20 kb
Edge clusters	Mean (SD)	8060 (452)	57.40 (1.83)	21.22 (2.94)	19.48 (1.73)	30.71 (3.15)	21.94 (1.89)	6.65 (1.70)
	CV	5.61%	3.19%	13.85%	8.90%	10.25%	8.62%	25.50%
Inner clusters	Mean (SD)	8258 (464)	57.20 (1.61)	19.83 (1.43)	19.08 (1.23)	30.11 (3.16)	23.57 (1.72)	7.40 (2.01)
	CV	5.62%	2.82%	7.23%	6.46%	10.49%	7.28%	27.13%
All clusters	Mean (SD)	8196 (464)	57.27 (1.61)	20.27 (1.43)	19.21 (1.23)	30.30 (3.16)	23.06 (1.72)	7.16 (2.01)
	CV	5.66%	2.82%	7.07%	6.42%	10.43%	7.44%	28.03%
AluI* & *HinfI								
Edge clusters	Mean (SD)	7809 (260)	55.76 (1.40)	19.15 (2.78)	20.53 (0.96)	32.48 (1.70)	22.23 (1.75)	5.62 (0.85)
	CV	3.33%	2.52%	14.50%	4.66%	5.24%	7.89%	15.15%
Inner clusters	Mean (SD)	7606 (221)	54.66 (1.24)	17.61 (2.76)	21.55 (0.91)	34.29 (1.73)	21.67 (1.60)	4.88 (0.65)
	CV	2.90%	2.27%	15.66%	4.20%	5.04%	7.38%	13.31%
All clusters	Mean (SD)	7659 (246)	54.95 (1.36)	18.01 (2.81)	21.28 (1.02)	33.81 (1.88)	21.82 (1.64)	5.08 (0.77)
	CV	3.21%	2.47%	15.62%	4.77%	5.57%	7.51%	15.18%
HinfI* & *MnlI								
Edge clusters	Mean (SD)	6648 (146)	55.91 (0.70)	18.81 (0.75)	28.62 (1.04)	34.30 (0.49)	15.36 (0.83)	2.91 (0.39)
	CV	2.20%	1.26%	4.01%	3.62%	1.43%	5.41%	13.38%
Inner clusters	Mean (SD)	6848 (283)	55.62 (0.79)	18.21 (0.82)	27.20 (1.67)	34.58 (0.45)	16.66 (1.74)	3.35 (0.77)
	CV	4.14%	1.42%	4.50%	6.15%	1.31%	10.43%	22.89%
All clusters	Mean (SD)	6793 (267)	55.70 (0.77)	18.37 (0.84)	27.59 (1.64)	34.50 (0.48)	16.30 (1.64)	3.23 (0.71)
	CV	3.98%	1.39%	4.57%	5.96%	1.38%	10.07%	21.93%
HphI* & *MnlI								
Edge clusters	Mean (SD)	6912 (204)	59.21 (0.69)	23.45 (1.25)	25.83 (1.03)	31.08 (0.73)	15.78 (1.03)	3.86 (0.57)
	CV	2.95%	1.16%	5.34%	4.00%	2.36%	6.56%	14.78%
Inner clusters	Mean (SD)	7064 (152)	59.33 (1.00)	23.92 (1.19)	24.54 (0.71)	30.42 (1.30)	16.98 (0.78)	4.14 (0.52)
	CV	2.15%	1.69%	4.99%	2.88%	4.27%	4.58%	12.49%
All clusters	Mean (SD)	7009 (182)	59.28 (0.89)	23.78 (1.21)	25.00 (1.02)	30.64 (1.16)	16.55 (1.03)	4.04 (0.54)
	CV	2.60%	1.50%	5.09%	4.08%	3.78%	6.21%	13.39%

Table 4. Inter-assay precision of repeated measurements, HinfI & MnlI digested DNA

DNA Sample ID		Telomere parameters		Frequency of telomeres, %				
		aTL (bp)	TLV, %	1–3 kb	>3–6 kb	>6–10 kb	>10–20 kb	>20 kb
8MIX1223	Mean (SD)	6897 (94)	61.08 (2.49)	18.26 (0.63)	26.33 (1.22)	35.17 (0.91)	16.99 (0.92)	3.24 (0.18)
	CV, %	**1.37%**	**7.75%**	**3.46%**	**4.63%**	**2.58%**	**5.42%**	**5.40%**
mTL1023	Mean (SD)	7501 (255)	64.01 (4.42)	18.72 (2.17)	23.30 (1.40)	32.63 (0.79)	20.05 (2.03)	5.29 (0.75)
	CV, %	**3.41%**	**6.91%**	**11.61%**	**6.00%**	**2.42%**	**10.12%**	**14.19%**
lTL1023	Mean (SD)	8536 (198)	66.25 (6.12)	19.52 (1.40)	18.22 (0.51)	28.99 (0.55)	24.66 (0.51)	8.60 (1.15)
	CV, %	**2.32%**	**9.24%**	**7.19%**	**2.80%**	**1.89%**	**2.08%**	**13.36%**

CVs were calculated from repeated measurements by DNA-array-FISH at THREE different time points.

Table 5. Reproducibility of TL measurements using UMUC3^{TERC} cell line DNA harvested at 7 passages (P0–P6)

		Telomere parameters		Frequency of telomeres, %				
		aTL (bp)	TLV, %	1–3 kb	>3–6 kb	>6–10 kb	>10–20 kb	>20 kb
Assay 1	Mean (SD)	6179 (1507)	66.42 (3.55)	23.64 (8.74)	25.21 (7.30)	28.90 (6.65)	17.39 (7.93)	4.87 (3.98)
Assay 2	Mean (SD)	6177 (1241)	64.79 (4.05)	23.66 (6.89)	24.21 (5.69)	29.73 (4.99)	17.87 (6.82)	4.52 (3.43)
	p-value*	0.99	0.23	0.98	0.21	0.36	0.38	0.20
	r^	1.00	0.65	0.99	0.99	0.97	0.99	1.00

DNA samples were digested with *HinfI* & *MnlI*. *Paired Student *t*-test, ^Pearson correlation co-efficient.

Table 5). There were no statistically significant differences in the other SIX telomere parameters. The correlation analysis indicates high reproducibility of the assay with Pearson correlation co-efficient (*r*) ranges of 0.97–1.00 for 6 out of 7 telomere parameters (aTL and percent of telomeres in the five TL groups, Table 5 and Figure 4). The correlation r of TLV is 0.65.

We further evaluated the reproducibility of the DNA-array-FISH method using DNA samples from human blood ($N = 92$). DNA samples were extracted using the Puregene genomic DNA kit from 53 buffy coats that were stored at –80°C for 3–8 years and 39 whole blood samples that were stored at –80°C for 15 years. DNA samples were digested with *HinfI* & *MnlI* restriction enzymes. The mean aTL of the 92 sam-

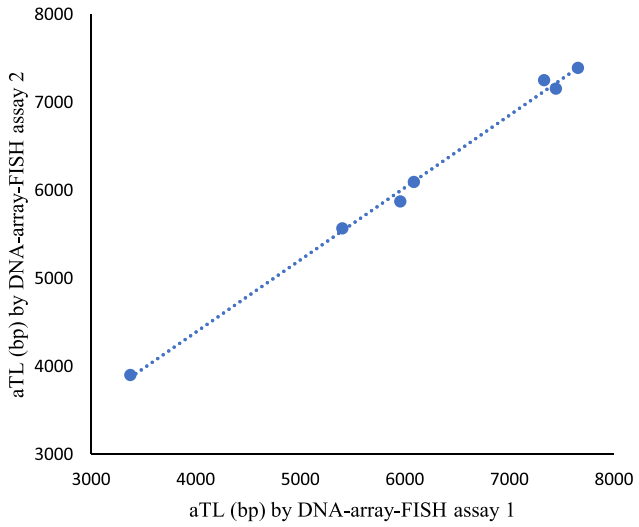

Figure 4. Correlation of aTL (bp) between repeated measurements ($r = 1.00$). DNA samples were extracted from cultured UMUC3^{TERC} cell lines harvested at seven passages (p0–p6) and were digested with *HinfI* & *MnlI*.

ples is 6743 and 6704 bp for assay 1 and assay 2, respectively ($P = 0.73$). The mean values of the other 6 telomere parameters were also similar and not statistically significant between the TWO measurements (Table 6) with one exception (percent of telomere in >6–10 kb group, $P = 0.03$). The correlation analysis confirms the high reproducibility of the assay with intraclass correlation co-efficient (ICC) ranges of 0.79–0.91 for all seven telomere parameters (Table 6 and Figure 5). The mean TL distribution of human blood DNA ($N = 92$) shows that about 52% of telomeres are in the range of 3–10 kb (Figure 2).

Comparison of aTL between DNA-array-FISH and TRF methods

TRF is regarded as the gold standard method for determining the aTL. To verify the accuracy of the DNA-array-FISH method, we compared aTL values between DNA-array-FISH and TRF using DNA samples of the UMUC3^{TERC} cell lines and two sets of DNA samples purified from human blood. UMUC3^{TERC} cell lines (85) that were harvested at seven passages (p0 – p6) were assayed by TRF using *HphI* & *MnlI* digestion (Supplementary Figure S1A) and by DNA-array-FISH using *HinfI* & *MnlI* digestion. The mean aTL of TRF (mean ± SD = 5176 ± 1198 bp) is significantly shorter than the aTL of DNA-array-FISH (mean ± SD = 6178 ± 1373 bp, $P < 0.001$). The aTLs of DNA-array-FISH are highly correlated with the aTLs of TRF ($r = 0.99$, Figure 6).

One set of 27 human blood DNA samples were extracted from buffy coats using the FlexiGene DNA kit and had been stored at –80°C for 12 years. aTL was measured by TRF using *HinfI* & *RsaI* digestion at Dr Aviv's lab at The State University of New Jersey (Supplementary Figure S3B) and by DNA-array-FISH using *HinfI* & *MnlI* or *HinfI* & *RsaI* digestion. The mean aTL of TRF assay (mean ± SD = 6766 ± 665 bp) is significantly longer than aTL of DNA-array-FISH of *HinfI* & *MnlI* digested DNA (mean ± SD = 6442 ± 674 bp, $P < 0.001$), but shorter than DNA-array-FISH of *HinfI* & *RsaI* digested DNA (mean ± SD = 7084 ± 733 bp, $P < 0.001$). The aTLs of DNA-array-FISH are highly correlated with aTLs of TRF, with $r = 0.90$ and 0.87 for *HinfI* & *MnlI* and *HinfI* & *RsaI* digested DNA, respectively (Figure 7).

The second set of 83 human blood DNA samples were extracted from peripheral blood mononuclear cells (PBMC) using the QiaAmp mini-DNA kit. aTL was measured by TRF using *HinfI* & *RsaI* digestion at Dr Aviv's lab at The State University of New Jersey and by DNA-array-FISH using *AluI* & *HinfI* digestion. The mean aTL of the TRF assay (mean ± SD = 7161 ± 780 bp) is significantly longer than the aTL of DNA-array-FISH (mean ± SD = 7004 ± 719 bp, $P < 0.001$). The aTL is highly correlated between TRF and DNA-array-FISH ($r = 0.88$, $P < 0.001$, Figure 8).

The relationship between telomere parameters and age

Previous studies have demonstrated that aTL in blood leucocytes is inversely correlated with age (86–88). We examined the correlation of aTL, frequency of telomeres and age in a set of 50 blood samples from donors with a mean age of 42.6 (range 19–83) years old. Using a median age of 41 as a cut point, means of telomere parameters were compared between young (≤41 years old) and old (>41 years old) age groups. We found that mean aTL is significantly longer in younger (mean = 6947 bp) than older (mean = 6438 bp, $P = 0.03$) age group (Table 7) and the frequency of short telomeres (TL = 1–3 kb) is significantly higher in the older than in the younger age group. In contrast, the frequency of long telomeres (TL > 10 – 20 kb) is significantly lower in the older than in the younger age group (Table 7 and Supplementary Figure S4). Age is inversely associated with aTL ($r = –0.37$), frequency of telomeres in >10–20 kb TL group ($r = –0.42$) and positively associated with frequency of telomeres in 1–3 kb TL group ($r = 0.37$) and >3–6 kb TL group ($r = 0.39$). Linear regression estimated the rate of aTL change at –20 bp per year of increasing age ($P = 0.01$). We then examined the rate of telomere shortening by TL percentiles and found that long telomeres shortened faster than short telomeres (Figure 9). For example, telomeres at the 25th percentile length (mean TL = 1871 bp) shortened approximately 6 bp per year while telomeres at the 90th percentile (mean TL = 18 259 bp) shortened approximately 38 bp per year (Figure 9).

Telomere length distribution in cancer cell lines and normal human blood DNA

The bladder cancer cell line UMUC3 exhibited a significantly shorter average telomere length (aTL = 3639 bp) compared to normal human blood DNA (aTL = 6924 bp, $P < 0.001$). UMUC3 cancer cell line showed higher frequencies of telomeres in <3 kb length groups and lower frequencies in >6 kb length groups compared to normal blood DNA (Figure 10).

Overexpression of the TERC gene in cancer cell lines is known to increase aTL during *in vitro* culturing (85). However, the impact of TERC gene overexpression on the distribution of telomere lengths is not well understood. Our findings showed that upon TERC gene expression, the frequency of telomeres shorter than 1 kb rapidly decreased in passages 1–3, then began to increase again in passages 5–6 (Figure 11). The frequency of telomeres longer than 10 kb rapidly increased in the first three passages and stabilized by passages 5–6, maintaining at an elevated level. Notably, the frequency of telomeres longer than 20 kb, which typically comprise approxi-

Table 6. Reproducibility of TL measurements using human blood DNA samples ($N = 92$)

		Telomere parameters		Frequency of telomeres, %				
		aTL (bp)	TLV	1–3 kb	>3–6 kb	>6–10 kb	>10–20 kb	>20 kb
Assay 1	Mean (SD)	6743 (777)	67.14 (2.93)	20.82 (3.56)	28.10 (4.24)	31.98 (2.14)	15.46 (4.39)	3.64 (2.11)
Assay 2	Mean (SD)	6704 (728)	66.36 (2.83)	20.32 (3.01)	28.26 (4.16)	32.63 (1.95)	15.38 (4.30)	3.41 (1.90)
	P-value[a]	0.73	0.07	0.31	0.80	0.03	0.90	0.44
	r^	0.91	0.88	0.82	0.91	0.80	0.90	0.90
	ICC	0.90	0.90	0.81	0.91	0.79	0.90	0.90

[a]Paired Student *t*-test, ^Pearson correlation co-efficient, ICC = intraclass correlation co-efficient.
DNA samples were digested with *HinfI* & *MnlI*.

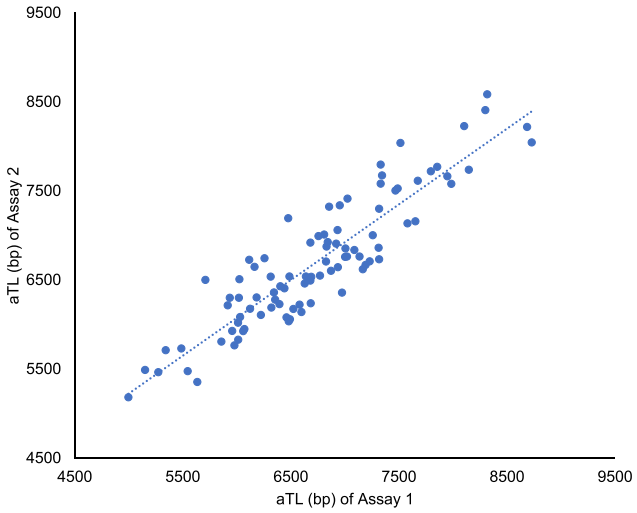

Figure 5. Correlation of aTL (bp) between repeated measurements by DNA-array-FISH of 92 human blood DNA samples (r = 0.91). DNA samples were digested with *HinfI* & *MnlI*.

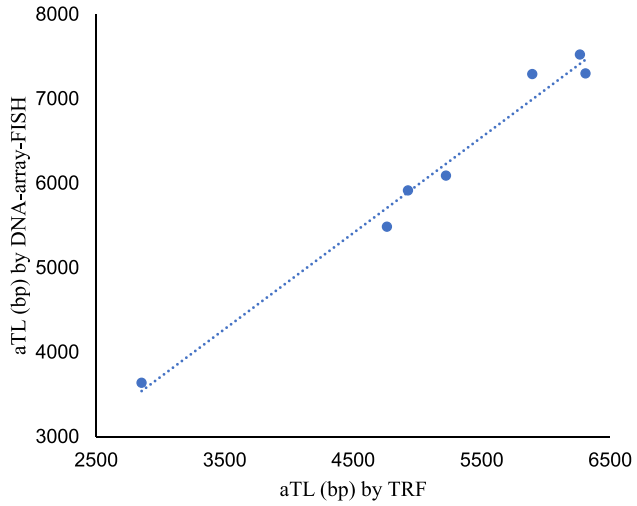

Figure 6. Correlation of aTL (bp) between TRF and DNA-array-FISH ($r = 0.99$). DNA samples were extracted from cultured UMUC3^{TERC} cell lines harvested at seven passages (p0–p6) and were digested with *HphI* & *MnlI* (TRF) or *HinfI* & *MnlI* (DNA-array-FISH).

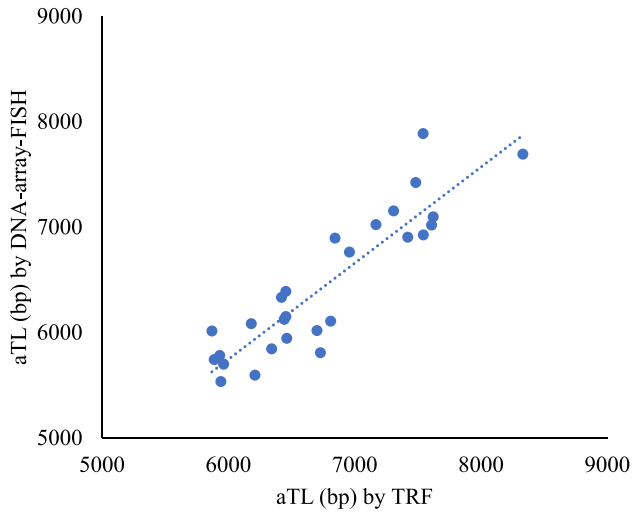

Figure 7. Correlation of aTL (bp) between TRF and DNA-array-FISH ($r = 0.90$). DNA samples ($N = 27$) were extracted from buffy coats and had been stored at –80°C for 12 years. DNA samples were digested with *HinfI* & *RsaI* (TRF) or *HinfI* & *MnlI* (DNA-array-FISH).

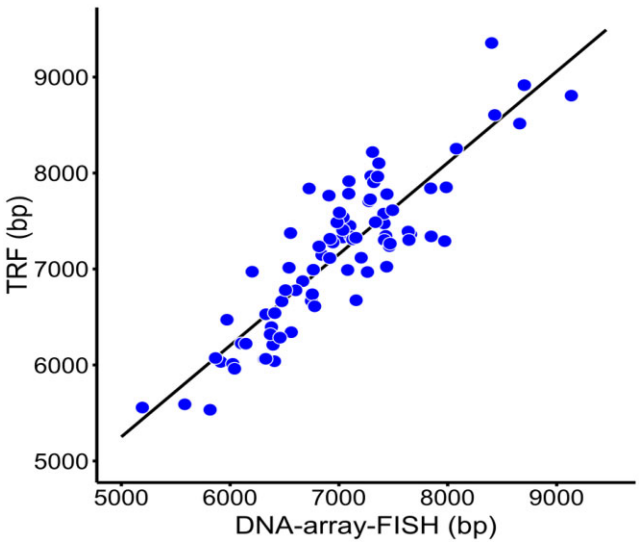

Figure 8. Average TL (bp) measured using DNA-array-FISH with *AluI* & *HinfI* digested DNA predicts aTL measured in the same samples using TRF with *HinfI* & *RsaI* digested DNA ($r = 0.88$).

mately 3% of the telomeres in normal human blood DNA, were increased to >7% in passages 4 and maintained at an elevated level in passages 5 and 6 of the UMUC3^{TERC} cell line (Figure 11). These additional insights into telomere length distribution may provide new avenues for studying telomere maintenance mechanisms in basic research.

Table 7. Association between telomere parameters in human blood and age ($N = 50$)

Age group	Telomere parameters		Frequency of telomeres				
≤41	aTL (bp)	TLV	1–3 kb	>3–6 kb	>6–10 kb	>10–20 kb	>20 kb
mean	6947	57.35%	19.44%	26.92%	32.69%	16.93%	4.02%
SD	749	2.44%	3.12%	4.04%	2.09%	4.30%	2.01%
>41							
Mean	6438	56.37%	21.67%	29.81%	32.04%	13.56%	2.92%
SD	843	3.03%	3.28%	4.65%	2.08%	4.57%	2.34%
P-value	0.03	0.22	0.02	0.02	0.27	0.01	0.08
r^a	–0.37	–0.25	0.37	0.39	–0.23	–0.42	–0.28

[a]Correlation with age, Pearson correlation co-efficient.
DNA samples were digested with *HinfI* & *MnlI*.

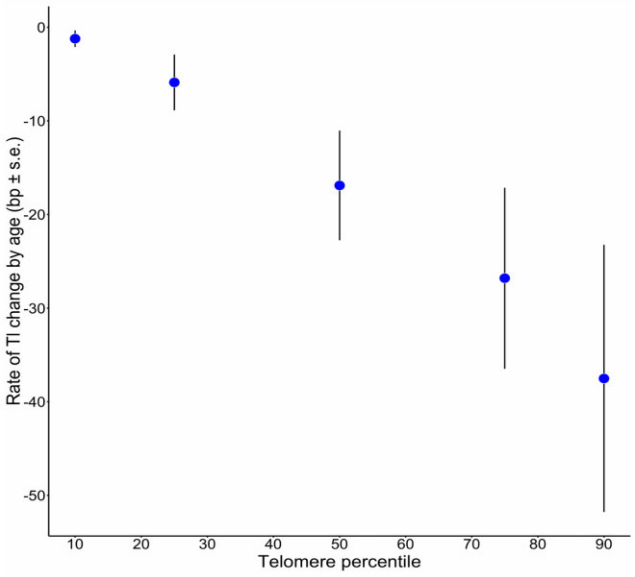

Figure 9. Effect of age on telomere length (mean bp/year ± SE) at different percentiles of telomere length.

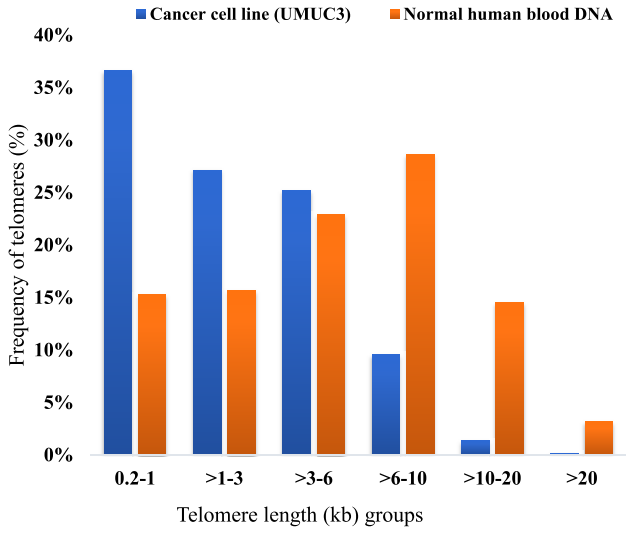

Figure 10. Telomere length distribution of a bladder cancer cell line, UMUC3, and a normal human blood DNA. DNA samples were digested with *HinfI* & *MnlI*.

Discussion

We report here the development of a DNA-array-FISH-based method to measure the bp lengths of single telomeres in a high-throughput process. This single telomere analysis method not only measures aTL, but also TL distribution and addresses the needs that are not met in population studies by current leading methods, namely q-PCR, TRF and Flow-FISH. The availability of a large number of single TL data (average 32000 telomeres per sample) provides an opportunity for an in-depth analysis of telomere dynamics and its relationship with aging-associated diseases at population level.

There are several advantages of the DNA-array-FISH method: (i) TL measurement at single telomere resolution allows generation of numerous telomere parameters, i.e. aTL, frequency of short telomeres or long telomeres, quintile length of telomeres etc., to fully characterize TL distribution; (ii) high precision for the measurement of aTL in bp. When restriction enzyme pairs of *HinfI* & *MnlI* or *AluI* & *HinfI* were used to digest the DNA, the intra-assay CV of aTL ranged from 3.21% to 3.98% (Table 3) and inter-assay CV of aTL ranged from 1.37% to 3.41% (Table 4). The correlation r of aTL in repeated measurements is in the range of 0.91–1.00; (iii) verified accuracy for the measurement of aTL by comparison to the current gold standard method, TRF. Correlation *r* of aTL between DNA-array-FISH and TRF are in the range of 0.87–0.99; (iv) high-throughput. Ninety-six DNA samples can be assayed in a single microarray chip and the cost of the assay is similar to q-PCR-based telomere assay; (v) requires a small amount (0.5 μg) of purified genomic DNA.

To achieve high technique precision, it is crucial to adhere to predetermined quality control and quality assurance (QC/QA) standards outlined in the method section. The telomere standard curve (TSC) serves the specific purpose of converting TL in FIU to TL in bp and mitigating assay variations across batches of chips assayed at different times. The TSC encompasses seven telomeric size standards ranging from 0.2 to 2.4 kb, a range shorter than aTL in the human genome (approximately 6.5 kb). Numerous attempts to clone longer telomeric fragments were unsuccessful in obtaining stable clones, thus an alternative approach was developed to improve the accuracy in estimating the slope and intercept of the TSC for TL conversion. In theory, if the estimated slope and intercept represent the true population mean values, then TL (bp) prediction will be accurate regardless the length of telomeres. Generally, a mean derived from a large random sample is more reliable in representing the true population mean than one from a small random sample. To enhance the accuracy of estimated slope and intercept values, we developed SCchips

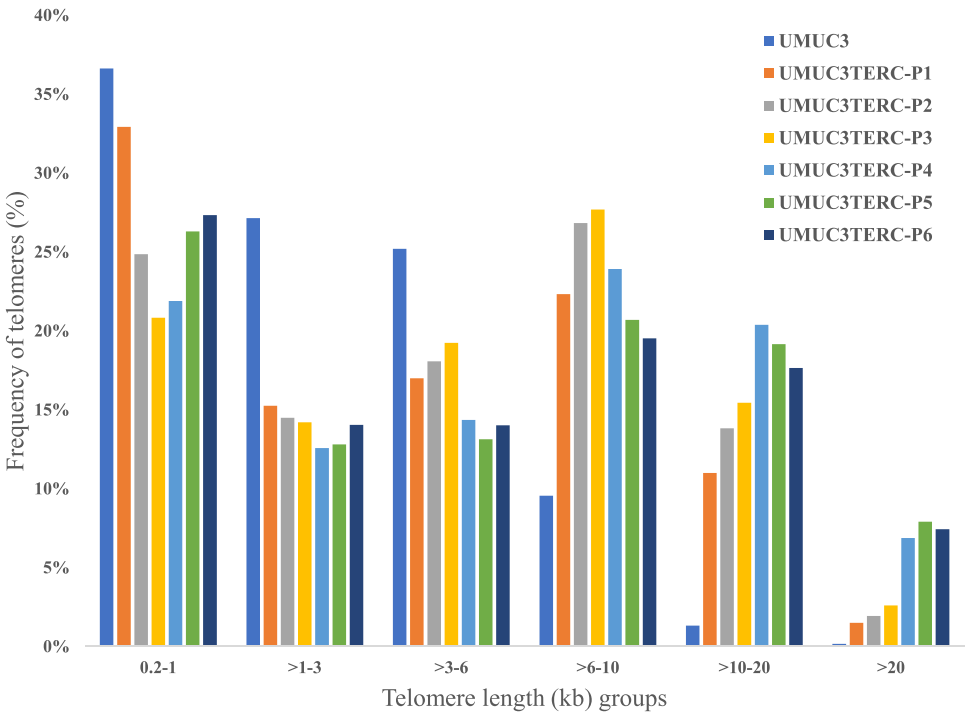

Figure 11. Telomere length distribution of bladder cancer cell lines: UMUC3 and UMUC3^{TERC}. UMUC3^{TERC} were harvested at passages 1, 2, 3, 4, 5 and 6. DNA samples were digested with *HinfI* & *MnlI*.

to generate a substantial number of TSCs, with 30 or more TSCs utilized to calculate mean intercept and slope values for TL conversion. This approach markedly improved assay precision, with inter-assay CV of aTL ranging from 1.37% to 3.41% when mean intercept and slope values from 30 TSCs were utilized for TL conversion, in contrast to observed inter-assay CV of 6–10% when intercept and slope values from a single on-chip TSC were applied (data not shown).

We found that the digestion of genomic DNA with restriction enzymes improved the quality and reproducibility of DNA microarray chips. Our data indicate that restriction enzyme digestion significantly affected the estimated aTL and TL distribution. *HinfI* & *RsaI*, the enzyme-pair most frequently used in TRF assay, showed higher technique variation (intra-assay CV of aTL ranges 5.61–5.66%) than *HinfI* & *MnlI* (intra-assay CV of aTL ranges 2.20–4.14%), *AluI*/*HinfI* (intra-assay CV of aTL ranges 2.90–3.33%), or *HphI* & *MnlI* (intra-assay CV of aTL ranges 2.15–2.95%). The estimated mean aTL of human blood DNA using *HinfI* & *RsaI* digestion is on average 1.1 kb longer than with *HphI* & *MnlI* or *HinfI* & *MnlI* digestion (Table 2) which is in agreement with the previously reported results by TRF assay (∼1 kb longer) (67). The differences between *HinfI* & *RsaI* and *HphI* & *MnlI* or *HinfI* & *MnlI* enzyme mixtures are that *HphI* & *MnlI* or *HinfI* & *MnlI* cut DNA within the sub-telomeric region, whereas *HinfI* & *RsaI* leave this region intact (67). Our data also indicate that the sub-telomeric regions that were removed by *HphI* & *MnlI* or *HinfI* & *MnlI* digestion contain largely the canonical telomere sequences that can be recognized by the telomere specific PNA probe. In addition to aTL, different enzyme mixtures drastically affect TL distributions (Tables 2 and 3). The variations in observed telomere length distributions between restriction enzyme digestions are associated with sub-telomeric regions that are complex and not well understood. The removal of sub-telomeric regions during restriction enzyme digestion depends on the specific cutting sites of the enzyme pairs within this region. This variability influences the size of the remaining sub-telomeric region and consequently affects the measurement of telomere length. Thus, it is critical to use the same restriction enzymes in a study or across epidemiological studies to facilitate comparisons and pooled data analysis.

It is crucial to underscore the significance of evaluating DNA integrity in telomere analysis. The accuracy and reliability of TL measurements are influenced by the quality of the DNA samples used. Previous studies investigated the impact of DNA quality on TL measurement using PCR and TRF methods, revealing that the integrity and quality of the DNA sample significantly affect the estimated TL (68,80), highlighting the need for stringent DNA quality control. Our study aligns with these findings, emphasizing the critical role of assessing DNA integrity prior to TL measurement. By ensuring high-quality DNA samples, potential biases and discrepancies can be minimized, thereby enhancing the reliability and validity of telomere data. However, in large population studies, conducting gel electrophoresis to analyze the DNA integrity of all samples may be prohibitively expensive. A trade-off procedure could be implemented to balance assay throughput and data quality. For example, gel electrophoresis could be performed on a randomly selected subset, such as 10% of samples. If this initial screening indicates that 1% of the samples do not meet the quality standard, then 1% or 2% of the samples showing the highest frequency of short telomeres (telomeres <1 kb in length) should undergo gel electrophoresis to ensure that the elevated frequency of short telomeres is not attributable to DNA degradation.

Limitations of DNA-array-FISH method: Although we observed high measurement precision for aTL (inter-assay CV

ranges 1.37–3.41%), the inter-assay variations for frequency of telomeres in 5 TL groups are variable (1.89–14.19%, Table 4). The inter-assay variations for the frequency of the shortest telomeres (1–3 kb) range between 3.46% and 11.61. The reason for this higher inter-assay variation may be attributed to: (i) a statistical effect of being based on a smaller number of telomeres; (ii) the variability in background signals that were counted as the shortest telomeres; (iii) out of focus telomeres at the edge of an image were included as short telomeres. We used the out of box MetaExpress image analysis software included with the microarray scanner. The software package does not allow for gating out telomeres located at the edges of digitized images that are not in sharp focus. Telomeres that are not in sharp focus could lead to lower and variable fluorescent intensity measurement and contribute to the higher measurement variation. Developing a better image analysis software to remove out-of-focus telomeres could improve the measurement precision of shortest telomeres and overall TL distribution. We also observed relatively high inter-assay variation for the frequency of the longest telomeres (TL > 20 kb) with CV ranging from 5.40% to 14.19% (Table 4), likely due to the low frequency of such excessively long telomeres in the human genome (average 3.52% in normal human blood samples, Table 6). The estimated overall telomere length variation (TLV) showed higher inter-assay variations (CV ranges 6.91–9.24%), reflecting the higher measurement variations of the shortest and longest telomeres since the value of TLV is largely driven by telomeres in these two extreme TL groups. Factors contributing to TLV include: (i) significant variations in telomere length among chromosomal ends, (ii) substantial variations in telomere length among cells at different points along the cellular aging continuum and (iii) measurement variations.

A microarray spotter and a fluorescent microscope imaging system are required to construct and scan microarray chips for this method. Since this equipment is often unavailable in typical research labs, it can be a barrier to adopting DNA-array-FISH-based telomere analysis. Given the method's high-throughput capabilities, setting up an institutional central laboratory, like a Shared Resource facility, could be a more practical solution to meet institutional or regional telomere analysis needs. Alternatively, using an industrial DNA-array-FISH telomere test provider, such as Contract Research Organization (CRO), is another option.

The DNA-array-FISH method detects canonical telomeric sequences longer than 200 bp in DNA samples, including telomeric sequences at chromosomal ends and interstitial telomeric sequences (ITS). In the human genome, canonical ITSs are well-defined and typically shorter than 100 bp (89,90). Therefore, we chose a 200 bp cutoff to minimize ITS detection in human DNA samples. When calculating aTL, we employed cutoffs of 2 kb for normal individuals and 1 kb for cancer cell lines. It is important to note that these cutoff values are somewhat arbitrary and may lead to an overestimation of aTL. In the future, improving the estimation of aTL may require refining these cutoffs through systematic bioinformatic approaches using extensive population data. Additionally, adjustments to TL cutoffs may be necessary when measuring TL in other species with different ITS structures in their genomes.

Previous studies have demonstrated that aTL in blood leucocytes is inversely correlated with age (86–88) and a recent meta-analysis of over 740 000 individuals estimates that the rate of TL change is –23 bp/year in cross sectional studies (87). Our data further confirmed that age is inversely associated with aTL of blood leucocytes ($r = -0.37$), with an estimated rate of aTL changes –20 bp/year, in agreement with previous reports. We also explored the rate of telomere shortening based on the length of telomeres and found that long telomeres, i.e. telomeres in the 90th percentile, shortened faster than short telomere, i.e. telomeres in the 10th percentile, per year of increasing age (Figure 9). Previous studies in birds reported that longer telomeres within a genome shortened faster with age and were better predictors of survival and fitness than shorter telomeres (91,92). This finding raised interesting questions about whether long telomeres are a better biomarker of 'life stress' because long telomeres better reflect cumulative effects of various stressors, such as oxidative stress and inflammation, than short telomeres, while shortest telomeres reflect telomere-induced cellular senescence (93). There is increasing evidence that telomere length exhibits a bi-directional relationship with risk of cancer and aging-associated diseases (94,95). For example, in a recent analysis of two large patient populations of over 216 000 individuals, both short aTL and long aTL of leucocytes showed an increased risk of death at a younger age (96). The analysis also identified that short leucocyte aTL was associated with 58 clinical phenotypes, such as liver cirrhosis and pulmonary fibrosis, and long aTL was associated with eight phenotypes that are all neoplastic in nature (96). These previous studies indicate a complex relationship between telomere dynamics and human aging and disease, highlighting the added value of single telomere analysis in future epidemiological studies.

In summary, we have developed a novel method to measure the telomere length in bp of individual telomeres using extracted genomic DNA. This method not only allows for the determination of aTL, but also facilitates the assessment of critically short or excessively long telomeres, TL distribution, and has the potential to advance our understanding of TL dynamics at the population level. This high-throughput, cost-effective approach will empower researchers to conduct comprehensive telomere research on a large population scale, leading to new insights that deepen our understanding of the intricate relationship between telomere biology and the risk of cancer and other age-related diseases. This method could also serve as a valuable tool for basic research. As depicted in Figure 11, detailed profiles of telomere changes in genetically manipulated cell lines could offer fresh insights into understanding telomere regulation mechanisms. Moreover, an accurate and affordable telomere length assay holds promise as a screening tool for the early detection of telomere-associated diseases.

Data availability

The data underlying this article will be shared on reasonable request to the corresponding author.

Supplementary data

Supplementary Data are available at NAR Online.

Acknowledgements

We are grateful for the following individuals and organizations for their support of this project: Survey, Recruitment and Biospecimen Collection shared resources at Georgetown

University Medical Center provided blood buffy coats samples and Telomere Research Network provided DNA samples extracted from PBMC for this study; TRF measurements of aTL in human blood samples were performed by Dr Abraham Aviv's laboratory at Rutgers New Jersey Medical School, The State University of New Jersey.

Funding

National Institute of Health [U01ES011786 to Y.L.Z., U01AG064785 to J.L.]; Georgetown University (to Y.L.Z.). Funding for open access charge: Georgetown University.

Conflict of interest statement

Y.L.Z. is the founder and holds equity in TelohealthDx LLC, a company dedicated to developing and commercializing telomere tests for both research and clinical applications. Other co-authors have declared no conflicts of interest.

References

1. Bodnar,A.G., Ouellette,M., Frolkis,M., Holt,S.E., Chiu,C.P., Morin,G.B., Harley,C.B., Shay,J.W., Lichtsteiner,S. and Wright,W.E. (1998) Extension of life-span by introduction of telomerase into normal human cells. *Science*, **279**, 349–352.
2. Calado,R.T. and Young,N.S. (2009) Telomere diseases. *N. Engl. J. Med.*, **361**, 2353–2365.
3. Callen,E. and Surralles,J. (2004) Telomere dysfunction in genome instability syndromes. *Mutat. Res.*, **567**, 85–104.
4. de Lange,T. (1998) Telomeres and senescence: ending the debate. *Science*, **279**, 334–335.
5. Finkel,T., Serrano,M. and Blasco,M.A. (2007) The common biology of cancer and ageing. *Nature*, **448**, 767–774.
6. Hahn,W.C. (2003) Role of telomeres and telomerase in the pathogenesis of human cancer. *J. Clin. Oncol.*, **21**, 2034–2043.
7. de Lange,T. (2018) Shelterin-mediated Telomere protection. *Annu. Rev. Genet.*, **52**, 223–247.
8. Meyne,J., Ratliff,R.L. and Moyzis,R.K. (1989) Conservation of the human telomere sequence (TTAGGG)n among vertebrates. *Proc. Natl. Acad. Sci. U.S.A.*, **86**, 7049–7053.
9. Levy,M.Z., Allsopp,R.C., Futcher,A.B., Greider,C.W. and Harley,C.B. (1992) Telomere end-replication problem and cell aging. *J. Mol. Biol.*, **225**, 951–960.
10. Olovnikov,A.M. (1973) A theory of marginotomy. The incomplete copying of template margin in enzymic synthesis of polynucleotides and biological significance of the phenomenon. *J. Theor. Biol.*, **41**, 181–190.
11. Lingner,J., Cooper,J.P. and Cech,T.R. (1995) Telomerase and DNA end replication: no longer a lagging strand problem?*Science*, **269**, 1533–1534.
12. Sfeir,A.J., Chai,W., Shay,J.W. and Wright,W.E. (2005) Telomere-end processing the terminal nucleotides of human chromosomes. *Mol. Cell*, **18**, 131–138.
13. Harley,C.B. (1991) Telomere loss: mitotic clock or genetic time bomb?*Mutat. Res.*, **256**, 271–282.
14. Krizhanovsky,V., Xue,W., Zender,L., Yon,M., Hernando,E. and Lowe,S.W. (2008) Implications of cellular senescence in tissue damage response, tumor suppression, and stem cell biology. *Cold Spring Harb Symp. Quant. Biol.*, **73**, 513–522.
15. Chakravarti,D., LaBella,K.A. and DePinho,R.A. (2021) Telomeres: history, health, and hallmarks of aging. *Cell*, **184**, 306–322.
16. Lansdorp,P.M. (2022) Telomeres, aging, and cancer: the big picture. *Blood*, **139**, 813–821.
17. Oeseburg,H., de Boer,R.A., van Gilst,W.H. and van der Harst,P. (2010) Telomere biology in healthy aging and disease. *Pflugers Arch.*, **459**, 259–268.
18. Rossiello,F., Jurk,D., Passos,J.F. and d'Adda di Fagagna,F. (2022) Telomere dysfunction in ageing and age-related diseases. *Nat. Cell Biol.*, **24**, 135–147.
19. Alder,J.K., Chen,J.J., Lancaster,L., Danoff,S., Su,S.C., Cogan,J.D., Vulto,I., Xie,M., Qi,X., Tuder,R.M., *et al.* (2008) Short telomeres are a risk factor for idiopathic pulmonary fibrosis. *Proc. Natl. Acad. Sci. U.S.A.*, **105**, 13051–13056.
20. Schafer,M.J., White,T.A., Iijima,K., Haak,A.J., Ligresti,G., Atkinson,E.J., Oberg,A.L., Birch,J., Salmonowicz,H., Zhu,Y., *et al.* (2017) Cellular senescence mediates fibrotic pulmonary disease. *Nat. Commun.*, **8**, 14532.
21. Schneider,J.L., Rowe,J.H., Garcia-de-Alba,C., Kim,C.F., Sharpe,A.H. and Haigis,M.C. (2021) The aging lung: physiology, disease, and immunity. *Cell*, **184**, 1990–2019.
22. Jeanclos,E., Krolewski,A., Skurnick,J., Kimura,M., Aviv,H., Warram,J.H. and Aviv,A. (1998) Shortened telomere length in white blood cells of patients with IDDM. *Diabetes*, **47**, 482–486.
23. Sampson,M.J., Winterbone,M.S., Hughes,J.C., Dozio,N. and Hughes,D.A. (2006) Monocyte telomere shortening and oxidative DNA damage in type 2 diabetes. *Diabetes Care.*, **29**, 283–289.
24. Verhulst,S., Dalgard,C., Labat,C., Kark,J.D., Kimura,M., Christensen,K., Toupance,S., Aviv,A., Kyvik,K.O. and Benetos,A. (2016) A short leucocyte telomere length is associated with development of insulin resistance. *Diabetologia*, **59**, 1258–1265.
25. Kitada,T., Seki,S., Kawakita,N., Kuroki,T. and Monna,T. (1995) Telomere shortening in chronic liver diseases. *Biochem. Biophys. Res. Commun.*, **211**, 33–39.
26. Wiemann,S.U., Satyanarayana,A., Tsahuridu,M., Tillmann,H.L., Zender,L., Klempnauer,J., Flemming,P., Franco,S., Blasco,M.A., Manns,M.P., *et al.* (2002) Hepatocyte telomere shortening and senescence are general markers of human liver cirrhosis. *FASEB J.*, **16**, 935–942.
27. Pignolo,R.J., Law,S.F. and Chandra,A. (2021) Bone aging, cellular senescence, and osteoporosis. *JBMR Plus*, **5**, e10488.
28. Valdes,A.M., Richards,J.B., Gardner,J.P., Swaminathan,R., Kimura,M., Xiaobin,L., Aviv,A. and Spector,T.D. (2007) Telomere length in leukocytes correlates with bone mineral density and is shorter in women with osteoporosis. *Osteoporos. Int.*, **18**, 1203–1210.
29. Fazzini,F., Lamina,C., Raschenberger,J., Schultheiss,U.T., Kotsis,F., Schonherr,S., Weissensteiner,H., Forer,L., Steinbrenner,I., Meiselbach,H., *et al.* (2020) Results from the German Chronic Kidney Disease (GCKD) study support association of relative telomere length with mortality in a large cohort of patients with moderate chronic kidney disease. *Kidney Int.*, **98**, 488–497.
30. Raschenberger,J., Kollerits,B., Ritchie,J., Lane,B., Kalra,P.A., Ritz,E. and Kronenberg,F. (2015) Association of relative telomere length with progression of chronic kidney disease in two cohorts: effect modification by smoking and diabetes. *Sci. Rep.*, **5**, 11887.
31. Boccardi,V., Pelini,L., Ercolani,S., Ruggiero,C. and Mecocci,P. (2015) From cellular senescence to Alzheimer's disease: the role of telomere shortening. *Ageing Res. Rev.*, **22**, 1–8.
32. Koh,S.H., Choi,S.H., Jeong,J.H., Jang,J.W., Park,K.W., Kim,E.J., Kim,H.J., Hong,J.Y., Yoon,S.J., Yoon,B., *et al.* (2020) Telomere shortening reflecting physical aging is associated with cognitive decline and dementia conversion in mild cognitive impairment due to Alzheimer's disease. *Aging (Albany NY)*, **12**, 4407–4423.
33. Boniewska-Bernacka,E., Panczyszyn,A. and Klinger,M. (2020) Telomeres and telomerase in risk assessment of cardiovascular diseases. *Exp. Cell. Res.*, **397**, 112361.
34. Fitzpatrick,A.L., Kronmal,R.A., Gardner,J.P., Psaty,B.M., Jenny,N.S., Tracy,R.P., Walston,J., Kimura,M. and Aviv,A. (2007) Leukocyte telomere length and cardiovascular disease in the cardiovascular health study. *Am. J. Epidemiol.*, **165**, 14–21.
35. Nassour,J., Schmidt,T.T. and Karlseder,J. (2021) Telomeres and cancer: resolving the paradox. *Annu. Rev. Cancer Biol.*, **5**, 59–77.
36. Telomeres Mendelian Randomization,C., Haycock,P.C., Burgess,S., Nounu,A., Zheng,J., Okoli,G.N., Bowden,J., Wade,K.H., Timpson,N.J., Evans,D.M., *et al.* (2017) Association between

telomere length and risk of cancer and non-neoplastic diseases: a mendelian randomization study. *JAMA Oncol.*, **3**, 636–651.
37. Shalev,I., Moffitt,T.E., Sugden,K., Williams,B., Houts,R.M., Danese,A., Mill,J., Arseneault,L. and Caspi,A. (2013) Exposure to violence during childhood is associated with telomere erosion from 5 to 10 years of age: a longitudinal study. *Mol. Psychiatry*, **18**, 576–581.
38. Willis,M., Reid,S.N., Calvo,E., Staudinger,U.M. and Factor-Litvak,P. (2018) A scoping systematic review of social stressors and various measures of telomere length across the life course. *Ageing Res. Rev.*, **47**, 89–104.
39. Pepper,G.V., Bateson,M. and Nettle,D. (2018) Telomeres as integrative markers of exposure to stress and adversity: a systematic review and meta-analysis. *R. Soc. Open Sci.*, **5**, 180744.
40. Zhang,X., Lin,S., Funk,W.E. and Hou,L. (2013) Environmental and occupational exposure to chemicals and telomere length in human studies. *Occup. Environ. Med.*, **70**, 743–749.
41. Zota,A.R., Needham,B.L., Blackburn,E.H., Lin,J., Park,S.K., Rehkopf,D.H. and Epel,E.S. (2015) Associations of cadmium and lead exposure with leukocyte telomere length: findings from National Health and Nutrition Examination Survey, 1999-2002. *Am. J. Epidemiol.*, **181**, 127–136.
42. De Vivo,I., Prescott,J., Wong,J.Y., Kraft,P., Hankinson,S.E. and Hunter,D.J. (2009) A prospective study of relative telomere length and postmenopausal breast cancer risk. *Cancer Epidemiol. Biomarkers Prev.*, **18**, 1152–1156.
43. Pooley,K.A., Sandhu,M.S., Tyrer,J., Shah,M., Driver,K.E., Luben,R.N., Bingham,S.A., Ponder,B.A., Pharoah,P.D., Khaw,K.T., *et al.* (2010) Telomere length in prospective and retrospective cancer case-control studies. *Cancer Res.*, **70**, 3170–3176.
44. Sanders,J.L., Fitzpatrick,A.L., Boudreau,R.M., Arnold,A.M., Aviv,A., Kimura,M., Fried,L.F., Harris,T.B. and Newman,A.B. (2012) Leukocyte telomere length is associated with noninvasively measured age-related disease: the Cardiovascular Health Study. *J. Gerontol. A Biol. Sci. Med. Sci.*, **67**, 409–416.
45. Zheng,Y.L., Ambrosone,C., Byrne,C., Davis,W., Nesline,M. and McCann,S.E. (2010) Telomere length in blood cells and breast cancer risk: investigations in two case-control studies. *Breast Cancer Res. Treat.*, **120**, 769–775.
46. Baird,D.M., Rowson,J., Wynford-Thomas,D. and Kipling,D. (2003) Extensive allelic variation and ultrashort telomeres in senescent human cells. *Nat. Genet.*, **33**, 203–207.
47. Bekaert,S., Derradji,H. and Baatout,S. (2004) Telomere biology in mammalian germ cells and during development. *Dev. Biol.*, **274**, 15–30.
48. Gomes,N.M., Ryder,O.A., Houck,M.L., Charter,S.J., Walker,W., Forsyth,N.R., Austad,S.N., Venditti,C., Pagel,M., Shay,J.W., *et al.* (2011) Comparative biology of mammalian telomeres: hypotheses on ancestral states and the roles of telomeres in longevity determination. *Aging Cell*, **10**, 761–768.
49. Lansdorp,P.M., Verwoerd,N.P., van de Rijke,F.M., Dragowska,V., Little,M.T., Dirks,R.W., Raap,A.K. and Tanke,H.J. (1996) Heterogeneity in telomere length of human chromosomes. *Hum. Mol. Genet.*, **5**, 685–691.
50. Hemann,M.T., Strong,M.A., Hao,L.Y. and Greider,C.W. (2001) The shortest telomere, not average telomere length, is critical for cell viability and chromosome stability. *Cell*, **107**, 67–77.
51. Liu,Y., Kha,H., Ungrin,M., Robinson,M.O. and Harrington,L. (2002) Preferential maintenance of critically short telomeres in mammalian cells heterozygous for mTert. *Proc. Natl. Acad. Sci. U.S.A.*, **99**, 3597–3602.
52. Bendix,L., Horn,P.B., Jensen,U.B., Rubelj,I. and Kolvraa,S. (2010) The load of short telomeres, estimated by a new method, Universal STELA, correlates with number of senescent cells. *Aging Cell*, **9**, 383–397.
53. Vera,E. and Blasco,M.A. (2012) Beyond average: potential for measurement of short telomeres. *Aging (Albany NY)*, **4**, 379–392.
54. Capper,R., Britt-Compton,B., Tankimanova,M., Rowson,J., Letsolo,B., Man,S., Haughton,M. and Baird,D.M. (2007) The nature of telomere fusion and a definition of the critical telomere length in human cells. *Genes Dev.*, **21**, 2495–2508.
55. Horn,S., Figl,A., Rachakonda,P.S., Fischer,C., Sucker,A., Gast,A., Kadel,S., Moll,I., Nagore,E., Hemminki,K., *et al.* (2013) TERT promoter mutations in familial and sporadic melanoma. *Science*, **339**, 959–961.
56. Seow,W.J., Cawthon,R.M., Purdue,M.P., Hu,W., Gao,Y.T., Huang,W.Y., Weinstein,S.J., Ji,B.T., Virtamo,J., Hosgood,H.D. 3rd, *et al.* (2014) Telomere length in white blood cell DNA and lung cancer: a pooled analysis of three prospective cohorts. *Cancer Res.*, **74**, 4090–4098.
57. Han,J., Qureshi,A.A., Prescott,J., Guo,Q., Ye,L., Hunter,D.J. and De Vivo,I. (2009) A prospective study of telomere length and the risk of skin cancer. *J. Invest. Dermatol.*, **129**, 415–421.
58. McNally,E.J., Luncsford,P.J. and Armanios,M. (2019) Long telomeres and cancer risk: the price of cellular immortality. *J. Clin. Invest.*, **129**, 3474–3481.
59. Bao,E.L., Nandakumar,S.K., Liao,X., Bick,A.G., Karjalainen,J., Tabaka,M., Gan,O.I., Havulinna,A.S., Kiiskinen,T.T.J., Lareau,C.A., *et al.* (2020) Inherited myeloproliferative neoplasm risk affects haematopoietic stem cells. *Nature*, **586**, 769–775.
60. Abdallah,P., Luciano,P., Runge,K.W., Lisby,M., Geli,V., Gilson,E. and Teixeira,M.T. (2009) A two-step model for senescence triggered by a single critically short telomere. *Nat. Cell Biol.*, **11**, 988–993.
61. Gu,P., Min,J.N., Wang,Y., Huang,C., Peng,T., Chai,W. and Chang,S. (2012) CTC1 deletion results in defective telomere replication, leading to catastrophic telomere loss and stem cell exhaustion. *EMBO J.*, **31**, 2309–2321.
62. Lustig,A.J. (2003) Clues to catastrophic telomere loss in mammals from yeast telomere rapid deletion. *Nat. Rev. Genet.*, **4**, 916–923.
63. Aubert,G., Hills,M. and Lansdorp,P.M. (2012) Telomere length measurement-caveats and a critical assessment of the available technologies and tools. *Mutat. Res.*, **730**, 59–67.
64. Montpetit,A.J., Alhareeri,A.A., Montpetit,M., Starkweather,A.R., Elmore,L.W., Filler,K., Mohanraj,L., Burton,C.W., Menzies,V.S., Lyon,D.E., *et al.* (2014) Telomere length: a review of methods for measurement. *Nurs. Res.*, **63**, 289–299.
65. Nussey,D.H., Baird,D., Barrett,E., Boner,W., Fairlie,J., Gemmell,N., Hartmann,N., Horn,T., Haussmann,M., Olsson,M., *et al.* (2014) Measuring telomere length and telomere dynamics in evolutionary biology and ecology. *Methods Ecol. Evol.*, **5**, 299–310.
66. Lai,T.P., Wright,W.E. and Shay,J.W. (2018) Comparison of telomere length measurement methods. *Philos. Trans. R. Soc. Lond. B Biol. Sci.*, **373**, 20160451.
67. Baerlocher,G.M., Vulto,I., de Jong,G. and Lansdorp,P.M. (2006) Flow cytometry and FISH to measure the average length of telomeres (flow FISH). *Nat. Protoc.*, **1**, 2365–2376.
68. Kimura,M., Stone,R.C., Hunt,S.C., Skurnick,J., Lu,X., Cao,X., Harley,C.B. and Aviv,A. (2010) Measurement of telomere length by the southern blot analysis of terminal restriction fragment lengths. *Nat. Protoc.*, **5**, 1596–1607.
69. Cawthon,R.M. (2002) Telomere measurement by quantitative PCR. *Nucleic Acids Res.*, **30**, e47.
70. Jasmine,F., Shinkle,J., Sabarinathan,M., Ahsan,H., Pierce,B.L. and Kibriya,M.G. (2018) A novel pooled-sample multiplex luminex assay for high-throughput measurement of relative telomere length. *Am. J. Hum. Biol.*, **30**, e23118.
71. Luo,Y., Viswanathan,R., Hande,M.P., Loh,A.H.P. and Cheow,L.F. (2020) Massively parallel single-molecule telomere length measurement with digital real-time PCR. *Sci. Adv.*, **6**, eabb7944.
72. Norris,K., Walne,A.J., Ponsford,M.J., Cleal,K., Grimstead,J.W., Ellison,A., Alnajar,J., Dokal,I., Vulliamy,T. and Baird,D.M. (2021) High-throughput STELA provides a rapid test for the diagnosis of telomere biology disorders. *Hum. Genet.*, **140**, 945–955.
73. Lai,T.P., Zhang,N., Noh,J., Mender,I., Tedone,E., Huang,E., Wright,W.E., Danuser,G. and Shay,J.W. (2017) A method for measuring the distribution of the shortest telomeres in cells and tissues. *Nat. Commun.*, **8**, 1356.

74. Beh,C.W., Zhang,Y., Zheng,Y.L., Sun,B. and Wang,T.H. (2018) Fluorescence spectroscopic detection and measurement of single telomere molecules. *Nucleic Acids Res.*, **46**, e117.
75. Karimian,K., Groot,A., Huso,V., Kahidi,R., Tan,K.T., Sholes,S., Keener,R., McDyer,J.F., Alder,J.K., Li,H., *et al.* (2024) Human telomere length is chromosome end-specific and conserved across individuals. *Science*, **384**, 533–539.
76. Schmidt,T.T., Tyer,C., Rughani,P., Haggblom,C., Jones,J.R., Dai,X., Frazer,K.A., Gage,F.H., Juul,S., Hickey,S., *et al.* (2024) High resolution long-read telomere sequencing reveals dynamic mechanisms in aging and cancer. *Nat. Commun.*, **15**, 5149.
77. Sanchez,S.E., Gu,Y., Wang,Y., Golla,A., Martin,A., Shomali,W., Hockemeyer,D., Savage,S.A. and Artandi,S.E. (2024) Digital telomere measurement by long-read sequencing distinguishes healthy aging from disease. *Nat. Commun.*, **15**, 5148.
78. Tham,C.Y., Poon,L., Yan,T., Koh,J.Y.P., Ramlee,M.K., Teoh,V.S.I., Zhang,S., Cai,Y., Hong,Z., Lee,G.S., *et al.* (2023) High-throughput telomere length measurement at nucleotide resolution using the PacBio high fidelity sequencing platform. *Nat. Commun.*, **14**, 281.
79. Holland,A.J. and Cleveland,D.W. (2009) Boveri revisited: chromosomal instability, aneuploidy and tumorigenesis. *Nat. Rev. Mol. Cell Biol.*, **10**, 478–487.
80. Lin,J., Smith,D.L., Esteves,K. and Drury,S. (2019) Telomere length measurement by qPCR - summary of critical factors and recommendations for assay design. *Psychoneuroendocrinology*, **99**, 271–278.
81. Martin-Ruiz,C.M., Baird,D., Roger,L., Boukamp,P., Krunic,D., Cawthon,R., Dokter,M.M., van der Harst,P., Bekaert,S., de Meyer,T., *et al.* (2015) Reproducibility of telomere length assessment: an international collaborative study. *Int. J. Epidemiol.*, **44**, 1673–1683.
82. Gutierrez-Rodrigues,F., Santana-Lemos,B.A., Scheucher,P.S., Alves-Paiva,R.M. and Calado,R.T. (2014) Direct comparison of flow-FISH and qPCR as diagnostic tests for telomere length measurement in humans. *PLoS One*, **9**, e113747.
83. Nakagawa,S., Johnson,P.C.D. and Schielzeth,H. (2017) The coefficient of determination R(2) and intra-class correlation coefficient from generalized linear mixed-effects models revisited and expanded. *J. R. Soc. Interface*, **14**, 20170213.
84. R Core Team (2021) A Language and Environment for Statistical Computing. *R Foundation for Statistical Computing*. Vienna,Austria, 4.1.3.
85. Li,S., Rosenberg,J.E., Donjacour,A.A., Botchkina,I.L., Hom,Y.K., Cunha,G.R. and Blackburn,E.H. (2004) Rapid inhibition of cancer cell growth induced by lentiviral delivery and expression of mutant-template telomerase RNA and anti-telomerase short-interfering RNA. *Cancer Res.*, **64**, 4833–4840.
86. Muezzinler,A., Zaineddin,A.K. and Brenner,H. (2013) A systematic review of leukocyte telomere length and age in adults. *Ageing Res. Rev.*, **12**, 509–519.
87. Ye,Q., Apsley,A.T., Etzel,L., Hastings,W.J., Kozlosky,J.T., Walker,C., Wolf,S.E. and Shalev,I. (2023) Telomere length and chronological age across the human lifespan: a systematic review and meta-analysis of 414 study samples including 743,019 individuals. *Ageing Res. Rev.*, **90**, 102031.
88. Lai,T.P., Verhulst,S., Savage,S.A., Gadalla,S.M., Benetos,A., Toupance,S., Factor-Litvak,P., Susser,E. and Aviv,A. (2023) Buildup from birth onward of short telomeres in human hematopoietic cells. *Aging Cell*, **22**, e13844.
89. Azzalin,C.M., Nergadze,S.G. and Giulotto,E. (2001) Human intrachromosomal telomeric-like repeats: sequence organization and mechanisms of origin. *Chromosoma*, **110**, 75–82.
90. Santagostino,M., Piras,F.M., Cappelletti,E., Del Giudice,S., Semino,O., Nergadze,S.G. and Giulotto,E. (2020) Insertion of telomeric repeats in the Human and horse genomes: an evolutionary perspective. *Int. J. Mol. Sci.*, **21**, 2838.
91. Bauch,C., Becker,P.H. and Verhulst,S. (2014) Within the genome, long telomeres are more informative than short telomeres with respect to fitness components in a long-lived seabird. *Mol. Ecol.*, **23**, 300–310.
92. Salomons,H.M., Mulder,G.A., van de Zande,L., Haussmann,M.F., Linskens,M.H. and Verhulst,S. (2009) Telomere shortening and survival in free-living corvids. *Proc. Biol. Sci.*, **276**, 3157–3165.
93. Grasman,J., Salomons,H.M. and Verhulst,S. (2011) Stochastic modeling of length-dependent telomere shortening in Corvus monedula. *J. Theor. Biol.*, **282**, 1–6.
94. Armanios,M. (2022) The role of telomeres in human disease. *Annu. Rev. Genomics Hum. Genet.*, **23**, 363–381.
95. Savage,S.A. (2024) Telomere length and cancer risk: finding goldilocks. *Biogerontology*, **25**, 265–278.
96. Allaire,P., He,J., Mayer,J., Moat,L., Gerstenberger,P., Wilhorn,R., Strutz,S., Kim,D.S.L., Zeng,C., Cox,N., *et al.* (2023) Genetic and clinical determinants of telomere length. *HGG Adv*, **4**, 100201.

Received: April 6, 2024. **Revised:** August 30, 2024. **Editorial Decision:** September 3, 2024. **Accepted:** September 9, 2024